SURGE PHENOMENA AT TRANSITION POINTS
ON TRANSMISSION LINES

by

GURDIP SINGH SARAN

A THESIS

submitted to

OREGON STATE COLLEGE

in partial fulfillment of
the requirements for the
degree of

MASTER OF SCIENCE

June 1956

APPROVED:

Professor of Electrical Engineering

In Charge of Major

Head of Department of Electrical Engineering

Chairman of School Graduate Committee

Dean of Graduate School

Date thesis is presented   2/2/56

Typed by June Hutchings

ACKNOWLEDGEMENT

The author takes pleasure in extending his gratitude to his major professor L. N. Stone for his guidance and encouragement during the project; to Professors A. L. Albert and R. Michael for the use of the equipment and to Professor F. O. McMillan for the photography of the apparatus and equipment.

Thanks are due my uncle, Mr. Basant Singh, for his moral and financial support.

TABLE OF CONTENTS

LIST OF FIGURES

TABLES

SURGE PHENOMENA AT TRANSITION POINTS
ON TRANSMISSION LINES

INTRODUCTION

When the current and voltage on a transmission circuit undergo
a change from one steady state to another, because of lightning,
switching operations, short circuits, line faults or other causes,
surges or traveling waves are set up which travel along the line
with approximately the speed of light. As the surges or the travel-
ing waves on a line reach a transition point at which there is an
abrupt change of circuit constants, such as an open or short-
circuited terminal, a junction with another line, or a transformer
or a machine winding, a part of the wave is reflected on the line,
and a part may pass to other sections of the circuit.

On the transmission lines and at the transition points speci-
fied above, the traveling waves exhibit a variety of phenomena. The
traveling waves are not only reflected and transmitted at the
transition point, but also attenuated and distorted. Thus, to
determine the current and voltage at any point along the line at a
certain time one must know the attenuation, distortion, and the
successive reflections. Though it is possible to study the surge
behavior at the transition points with a lattice, a space-time
diagram, by virtue of which the shape for all the reflected and the
refracted waves can be calculated along with the affects of
attenuation and distortion of waves, the mathematical approach can
be lengthy and tedious (28, pp. 144-176). For the sake of simplicity

it was intended to study visually the surge phenomena as they appear on the artificial transmission lines.

During the past few years several tests have been made with the high voltage impulse generators which can produce standard lightning impulses on the actual power transmission lines (12, pp. 569-576). The purpose of the tests has been to study the insulation strength of the machine and transformer windings and also to investigate the surge severity at the junction of two or more transmission lines. The practice in the past has been to be on the liberal side concerning the insulation level and the protection of the machine and transformer windings without full attention to the actual severity of the surges. While these tests are being performed on the actual power systems, it was enlightening to set up some such system on a much smaller scale for tests in the laboratory.

This project deals with the investigation of voltage and current phenomena at the transition points on the artificial power transmission lines when a lightning impulse is applied at a point on one of the transmission lines with a miniature surge generator. To observe and photograph the waveforms a high-speed oscilloscope was utilized. The limitations of the artificial transmission line with reference to the standard lightning impulse which consists of different frequency components are kept in mind throughout the test.

The major portion of this study falls under two different categories as follows:

Surge generators and the lightning impulses.

Transmission lines.

THE SURGE GENERATORS AND THE LIGHTNING IMPULSES

Though our power systems can be thrown out of stability with switching or other faults, lightning is the most severe of all transient phenomena. Protection is secured against direct strokes by the use of ground wires over the power conductors. The ground wires are so placed as to intercept direct strokes within at least half a mile of the substations. The ground wires are grounded at each tower. Further protection from lightning is secured by the use of lightning arresters, which act as safety valves in passing excess charge from line conductors to ground and resume their insulating characteristics after the stroke.

The Lightning Impulses

The lightning impulses as recorded in the field with the lightning masts are not necessarily the same as encountered on the transmission lines. Some strokes might stay as they normally would, but others are intercepted and chopped. The waveforms can be listed under three different classifications (12, pp. 569-576):

>short-tail,
>
>chopped wave, and
>
>full wave.

Short-tail wave. The short-tail waves result from high-current

strokes to the shielding system followed by an insulator string flash-over which raises the phase conductor to tower-top potential. The short-tail is primarily due to the loss of the $L \frac{di}{dt}$ component of voltage at the struck tower after the current reaches its maximum. A typical value of the tower inductance is 20 microhenrys with a coupling factor of approximately 25% between the ground wire and the phase conductors, and the tower footing resistance is nearly 10 ohms (12, pp. 569-576).

Chopped waves (on front). Chopped waves result from the strokes directly to the phase wire of sufficient magnitude to flashover the insulation to the tower. The wavefront lasts until the insulators flashover. After that, the low resistance of the tower footing diverts the wave to the ground. These waves occur more than half as frequently as the short-tail waves.

Full waves. Full waves are of low current magnitudes. They result from a direct stroke to the conductor on which the insulators do not flashover because of the low values of voltage. Though the full waves are less frequent than the above two, they cause severe damage because of the long tail.

In general practice experimenters deal with the short-tail and full waves because of the frequency of occurrence and the severity, respectively.

Recommendations for Impulse Voltage Testing

In 1933 the Committee recommended that the impulse strengths of
the insulation etc. be determined from tests made with the following
3 waveshapes (21, 466-474):

> 1/5 microseconds,
>
> 1/10 microseconds, and
>
> 1.5/40 microseconds.

The above three waveforms cover a wide range to meet the require-
ments of simulated lightning. The Committee neglected wavefronts of
less than 1 microsecond because of the difficulty of obtaining them
at higher voltages. The transformer subcommittee of the electrical
machinery committee has selected tentatively 1.5/40 microseconds wave
for impulse tests for the transformers. In England, 1/50 microseconds
waveshape is regarded as the standard impulse for testing purposes
(9, p. 155).

As discussed previously, the lightning impulses vary considerably.
Therefore, it is not surprising to note that for testing purposes,
impulses of waveforms other than 1.5/40 microseconds are used
commonly. A 10/50 microseconds waveshape was used to test generator
windings (20, pp. 123-31), the reason being that very steep wavefront
waves may concentrate the complete voltage of the impulse across a
few turns, thus overstressing the turn insulation. However, when the
wavefront is 10 microseconds, the stress may be distributed over all
the winding turns thus releasing them of the overstress. Shorter
waves like 1/5 microseconds with $\pm$ 50% tolerance on the wave front

6

and $\pm$ 20% on the wavetail are also allowed for tests.

Definition of the Wavefront and the Wavetail of an Impulse

The symbol such as 1.5/40 microseconds means that the wavefront is 1.5 microseconds long while the wavetail lasts 40 microseconds. The wavefront is the time required for an impulse to rise from its approximate zero point to its peak. The wavetail is the time from the start to the point where the waveform has reduced to half of its peak magnitude. (See reference 9, pp. 155-157).

The Actual Surge Generators

The impulse generator is used to produce high-voltage impulses which in turn are utilized to test the insulation properties of the transmission and distribution lines apparatus. The mechanism of an impulse generator consists of a set of capacitors, resistors, rectifiers, and transformers, etc. by means of which high-voltage impulses of different wavefronts and wavetails can be produced. The process is the charging of capacitors in parallel with a d.c. source and discharging them in series through load. Some companies have built these big impulse generators which can produce waveforms of the order of several thousand kilovolts. A 2,000 KV impulse generator built by Metropolitan-Vickers Electrical Company has 12 stages, each of 0.12 μ F capacitance. The discharge capacitance is therefore 0.01 μ F and the discharge energy is 20,000 joules. The d.c. charging voltage is 167 KV (4, pp. 135-139). These figures obviously indicate

that the physical size of such a generator is very large and also
that the generators are costly. Therefore, it was necessary to
build a miniature surge generator, the characteristics of which dupli-
cate the functions of the large generator except for the magnitude of
voltage and current.

E. Marx is considered the pioneer in the field of impulse genera-
tors. His first circuit was only a voltage-doubling circuit, but
later he extended his circuit to an eight-stage generator. Later
Mr. Goodlet modified Marx's circuit so the load could be grounded
during the charging period without the necessity for an isolating
gap. The modern multi-stage circuit (9, pp. 155-180) with distributed
series resistors to give maximum efficiency has been developed by
Edwards and Scoles.

Most of the recently-built impulse generators use oil-impregnated
capacitors in insulating containers. The capacitors have the
dielectric assembled in an insulating cylinder of porcelain or
varnished paper with plane metal end-plates. The advantage of this
system is that successive stages of capacitors can be built up in
vertical columns, each stage being separated from the adjacent one
by supports of the same form as the capacitors but without the
dielectric (4, pp. 133-135).

The measurements of the impulse voltages can be made with sphere
gaps and capacitance-type voltage dividers for chopped waves, and
with R,L,C repeated-structure networks for all frequencies and wave-
forms (6, pp. 571-583).

A single-sweep oscillograph used with a potential divider is the most satisfactory method for examining waveshapes. Because of the short duration of the waves it is necessary that the operation of the generator and the oscilloscope be synchronized accurately; and if the wavefront is to be recorded satisfactorily, the oscillograph time sweep must be initiated at a time slightly before the impulse wave reaches the deflecting plates.

The miniature surge generator is of significant assistance in making the preliminary determination of the constants which affect the waveshape. This instrument enables the operator to determine the constants to be used in the large generator to obtain the proper waveshape. As mentioned previously the small generator duplicates the functions of the large generator with the exception of current and voltage magnitudes only.

The Miniature Surge Generator

The circuit diagram for the miniature surge generator is shown in Figure 1. Before going into the actual operation of the circuit as a whole, it will be of interest to study the effect of R_1, R_2, C_1 and C_2 on the production of the waveforms.

Theoretically, it has been proved that when R_2 is on the load side of R_1, a lower output voltage is obtained because the two resistors form a potential divider (9, pp. 155-156). The voltage efficiency can be improved by putting R_2 on the generator side of R_1, but practically it cannot be done because the resistance of the

120 V
60 ~
F. SW
FUSES
H.V. SW
T. SW

PL
PL
PL

1:4
1:2
4:1

V

1K
836
C₁
0·03   0·05
FG 33
R₁
R₂   C₂
OUTPUT

36K   884
0·1 M
0·1   C₃   0,1M
470
240
→ TRIGGER FOR SCOPE

10K   1M
10K   ,0·1

25   50

Key:
F. Sw.   Filament switch
H.V.Sw.   High voltage switch
T. Sw.   Triggering switch
P.L.   Pilot light

Note - The indicated
   capacitor values
   are in
   microfarads.

5·5   100   200   300

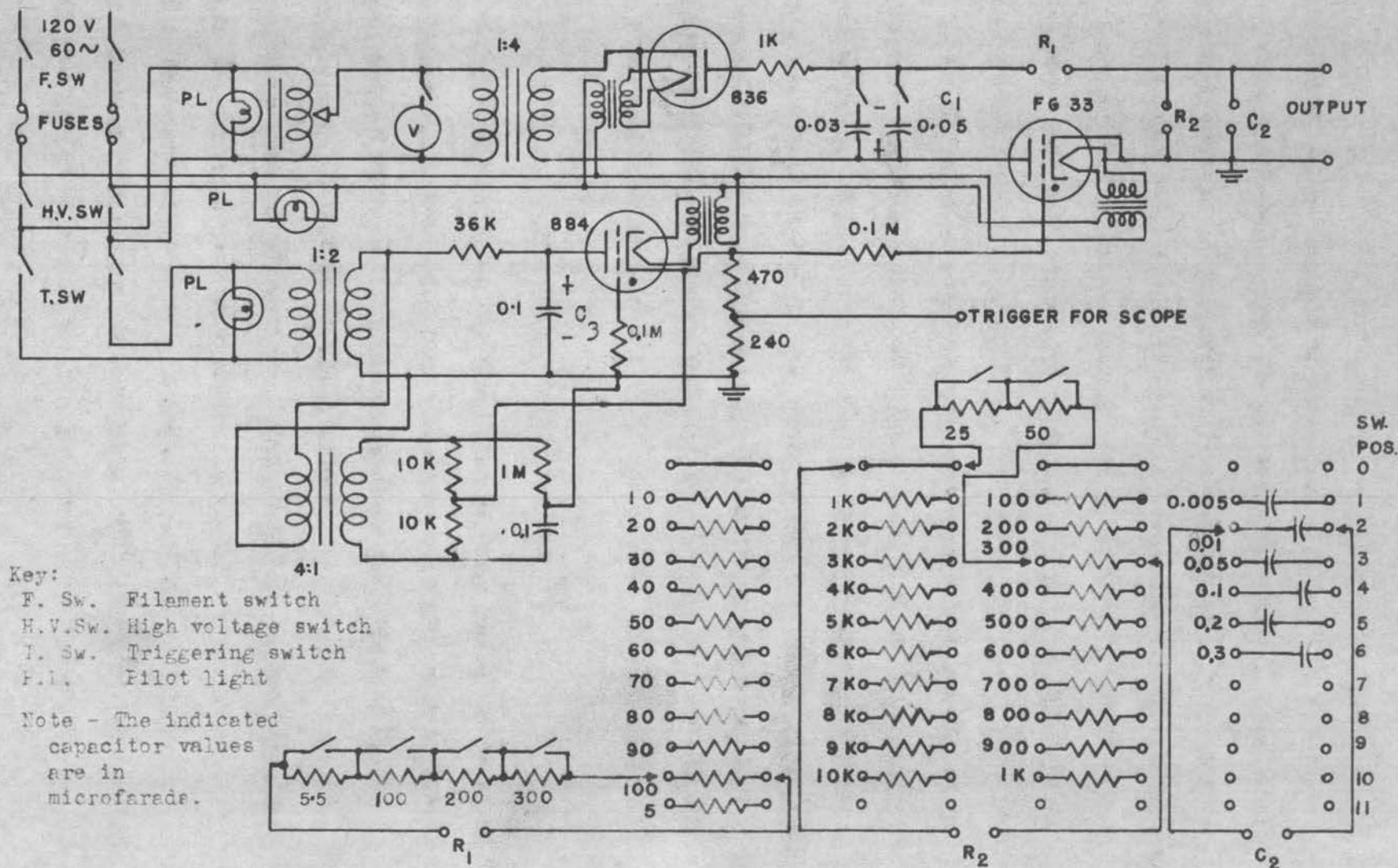|	R₁		R₂			C₂	SW. POS.
				100			0
10		1K	100		0.005		1
20		2K	200				2
30		3K	300		0.01 0.05		3
40		4K	400		0.1		4
50		5K	500		0.2		5
60		6K	600		0.3		6
70		7K	700				7
80		8K	800				8
90		9K	900				9
100		10K	1K				10
5							11

R₁   R₂   C₂

Fig. 1. The circuit diagram for the impulse generator.

6

thyratron is always present in the circuit.

Though it is very difficult to determine exactly the effect of varying resistors or capacitors on the waveform, it can be generalized that the series resistor R_1 controls the wavefront, while the resistor R_2 dominates the variations in the wavetail (25, pp. 169-176, 26, pp. 183-189). For better efficiency, the generator capacitor C_1 is kept larger than C_2 (9, pp. 155-156).

In the case of inductance in series with R_1, the mathematical analysis becomes enormously difficult; and the presence of the inductance may sharpen or flatten the waveform depending upon its value and also upon the waveform (9, p. 130). For the derivation of the equations for this circuit see reference 9, pp. 117-129; the final results are given in the Appendix.

The operation of the circuit for the miniature surge generator can be explained as follows: The capacitors C_1 and C_3 charge with the indicated polarities during the same half cycle of the sine wave. During the next half cycle of the sine wave, the capacitor C_3 discharges through the thyratron 884 which in turn is triggered by a phase-shifted sine wave. The discharge time of the capacitor C_3 is controlled by the resistors valued 470 and 240 ohms and also by the resistance of the thyratron 884. The waveform of the triggering impulse for the thyratron FG-33 is shown in Figure 21. The same triggering impulse but with lower voltage magnitude is used for the oscilloscope. The voltage magnitudes of the triggering impulses for the thyratron FG-33 and the oscillograph are nearly 150 volts and 50

volts (peak), respectively.

It was noticed that the thyratron FG-33 can also be triggered with an impulse of 50 volts peak, but the ionization time was over 15 microseconds with the normal operating voltages of the circuit. The long ionization time makes it impossible to watch the wavefront on the oscillograph when its sweep time is fast. For that reason, it was desirable to apply to FG-33 an impulse of higher voltage magnitude to cut down the ionization time.

The 36 K resistor (adjacent to C_3) in Figure 1 takes the place of a diode. The function of a diode in a circuit of this type is to let the capacitor charge during one half cycle and to block it from discharging during the next half cycle. Though 36 K resistor cannot fully stop the discharge of C_3 during the desired period, the discharge is slow because of the long time constant. Therefore, by the time thyratron 884 fires, C_3 has sufficient voltage across it to produce impulses of the desired voltage magnitude. The value of 36 K for the resistor gave approximately the best results.

Since the thyratron 884 has negative characteristics, the R-C phase shifting circuit shifts the negative half cycle of the sine wave by approximately 90 degrees so that the thyratron will not fire during the charging period of the capacitor C_3. The fact that polarity of the output impulse waveforms of Figure 1 is negative rather than positive needs an explanation. In order to produce a positive impulse one must remove the ground from the cathode of FG-33 and ground the load side of R. Moreover, the triggering circuit has to

be ungrounded to avoid a short circuit if the triggering impulse is to be applied between the cathode and the grid of FG-33. The above-mentioned procedure fails to give stable results because the cathode is not fixed with respect to any reference point, and the stray capacitance of the circuit gives rise to the uncertainties of the operation. Another alternative is to connect the FG-33 thyratron in such a way that the plate is towards the load and the cathode towards the source; then the polarity of the rectifier 836 has to be reversed. Here again the cathode cannot be grounded. The third alternative is to interchange R_1 and FG-33 with its cathode towards the load side; again a negative impulse is obtained if the cathode is grounded. Therefore, the present arrangement of Figure 11 seems to be the best in spite of negative output because the cathode is grounded; it results in the minimum interelectrode capacitance on the ground side, and the stray capacitance of the circuit does not alter the operation of the circuit.

The impulse generator, its top view and its bottom view, are shown in Figures 2, 3 and 4, respectively.

On the actual impulse generators, it becomes fairly difficult to produce the desired waveform across a given load. If the test object has low capacitance (not more than 1000 micromicrofarads), RC circuit is satisfactory; if the capacitance is much larger than that, it might be necessary to insert an inductor in series with the series resistor and remove the capacitor C_2 (18, pp. 35-37). The cables have very high capacitance (0.2 microfarads for 200 yards length) and
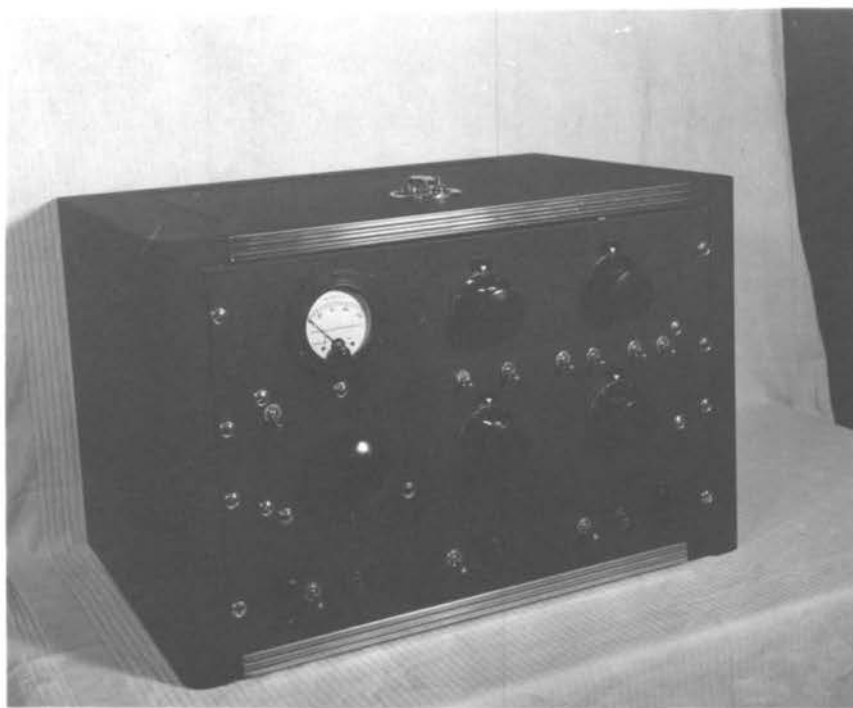
13

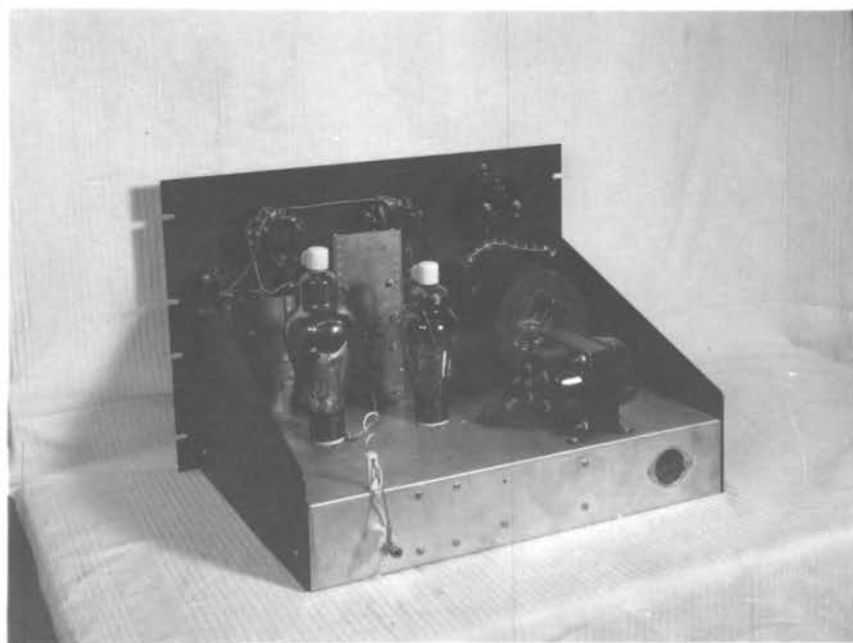Fig. 2. The impulse generator.

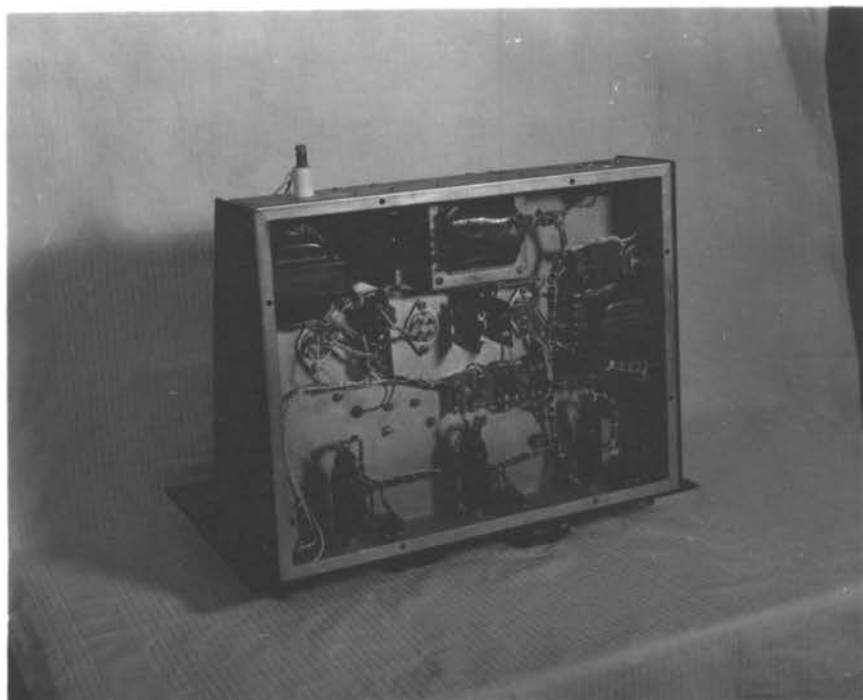Fig. 3. The top view of the impulse generator.

Fig. 4.   The bottom view of the impulse generator.

Fig. 5.   The apparatus.

hence require surge generators of very high capacitance which are
physically impossible. The long cables can be tested (d.c. test)
by using selenium rectifiers where the main capacitance comprises a
few drums of cables which can be charged to a desired potential
(2, pp. 684-685).

Certain advantages and many applications of the miniature surge
generators cannot be overlooked. The small surge generators are an
excellent guide for the setting of constants on the big impulse
generators. These small generators can be used on small impedance
loads because of their low internal impedance. They can also detect
winding fault in a very short time and with no loss to insulation
because of low output voltages (17, pp. 376-383). The surge genera-
tors can also be used to produce certain waveshapes and are used to
calibrate other instruments for measuring the complex waveforms. One
such application is for the calibration of ignition crest voltmeters
with a surge generator which is built to put out a pulse similar to
the output of the ignition output (7, pp. 99-104).

THE TRANSMISSION LINES

The Comparison Between the Artificial and the Real Lines

It is highly desirable to be able to duplicate the electrical
behavior of actual transmission lines on the artificial lines. The
artificial lines can be used as miniature transmission lines or as
pulse or time-delay circuits in radar and television systems.

An artificial line made of π or $\top$ sections resembles a real line

more closely the more sections the former has for a certain line length. If the artificial line is to be required to give fair equivalence to a real line for a wide band of frequencies, it then has to be made of small sections connected in series. Though a line composed of distributed constants gives a true representation of a real line at one frequency only, its circuit resembles that of a low-pass filter (23, p. 179). The equivalence of the artificial transmission lines to an actual line will be taken up later on, but it is to be emphasized here that if the number of sections used to represent a real line is increased without limit, the size of each section becoming smaller and smaller as the number is increased, the artificial line approaches an exact representation of the real line.

Next, the arrangement of the sections is discussed and the comparison between the artificial and the actual transmission line is made.

On an actual transmission line, the constants or the parameters are distributed and consist of inductance capacitance, resistance, and leakance. When one takes these constants into consideration, the line can be represented with either π or T sections (28, pp. 112-113).

The lumped line loses its close equivalence to the actual line (especially for surges) when the flow of current is not a repeating function. The constants behave as separate units toward the wave-fronts set up in changing from one state of flow to another, resulting in very large reflections from the lumped inductance and

very large conduction by the lumped capacitance. If the inductance
were entirely free from distributed capacity, then a vertical wave-
front would be completely reflected. However, the inductance coil
must always contain a certain amount of distributed capacity and
therefore the reflection of a wavefront will depend upon the ratio
of the inductance to the actual distributed capacity. Since the
distributed capacity of the coils is not designed but occurs as a
result of winding wire in a coil, it is a more or less poor feature
of the usual artificial line. The waves resulting from a transient
impressed upon a lumped line consist of a multiplicity of super-
imposed reflections which can distort it from its correct form. In
this case, the best thing to hope for is that the line has just about
the same amount of the distributed capacitance all along it. In
order to avoid superimposed reflections, it is highly desirable to
make an artificial line for which the inductance and capacitance
are intimately associated at all points in a similar manner as
they exist actually on the real lines (8, pp. 803-823).

Several years ago, Massachusetts Institute of Technology made
some artificial transmission lines to study the transient phenomena.
Their coils consisted of tinfoil wound between the different layers
of wire and insulated from the winding by the usual form of condenser
dielectric paper. Each layer of tinfoil projected at one end so that
all the layers were soldered together. This resulted in a coil having
the capacity uniformly distributed along the conductor. The
formulas were derived to calculate this capacitance for a certain

coil and necessary steps were taken to manufacture the coils within reasonable tolerance. The reason for directing attention to such intricate design was to be able to build transmission lines of several hundred miles in few sections (8, pp. 803-823). For this project, satisfactory results were obtained by using 0.73 mile sections to be described later on.

As brought out previously, an artificial transmission line is equivalent to actual transmission at one frequency. The artificial transmission line is a low-pass filter. If the cut-off frequency is remote from the operating frequencies, the discrepancies for the different frequencies are very slight—such is not the case in practice. The high frequencies occur partly because of the period of the reflection or oscillation of high frequency components and partly because of the steep wavefront which consists of many frequency components. On an artificial line there is a certain amount of periodicity because of the mutual inductance between turns in each coil being lumped with the coils.

It is of interest to notice that skin effect is almost entirely absent in artificial line coils. This fact is quite obvious on the actual transmission lines at higher frequency components of the surge because of the larger diameter of the conductors.

Since the lightning surges on transmission lines are of very high voltages and currents, corona is predominant on the lines in the vicinity of lightning stroke. Corona tends to attenuate and distort the top of the wave as it progresses along the line (1, p. 36).

There are many other minor losses on the actual transmission lines not exactly simulated in the laboratory on the artificial lines. These losses include dielectric losses in the insulation, radiation loss at very high frequencies or for steep wavefronts and leakages over the insulators.

From the above discussion, it is quite apparent that it is impossible to simulate a line with exact electrical characteristics of a real line except for the real line in the field itself. It is not, however, the purpose of this project to strive for exact reproduction of a transmission line, but only to study the different phenomena with approximations.

The Artificial Transmission Line

An attempt was made to make the parameters (R, L, C, and G) of the artificial line closely resemble those of a practical line. To cite a practical case, there is associated with Hoover dam a transmission line approximately 175 miles long. The transmission line uses a 795,000 circular mills conductor with spacing of 25 feet between conductors and with the outside diameter of conductor being 1.108 inches. The above-mentioned transmission line has its parameters as follows:[1]

---

[1]Starr, E. C., Class lectures at Oregon State College, Corvallis, Oregon (1954).

$r = 0.115$ ohm per mile, each wire

$l = 0.002125$ henry per mile, each wire

$c = 0.01369$ microfarad per mile, each wire

$g = 0$

A little thought concerning the design of the coils will indicate that it is very expensive to wind small coils with resistance comparable to that of an actual line. It is easier to approach an equivalent resistance condition by making a coil bigger, but then (as has already been pointed out) one deviates further from the representation of an actual transmission line. Moreover, the resistance of the line is not of much importance for an impulse because the attenuation due to resistance is negligible as compared to the magnitude of the impulse and also in comparison to the reflections on the line in the case of a mismatch. The general trend is to consider only the inductance and capacitance when dealing with the lightning impulses (20, pp. 123-131).

For this experiment the values of the capacitors available for use were also a controlling factor for the determination of the section lengths. Since they were 0.01 microfarads, everything else had to be planned accordingly. The parameters should be as follows:

$c = 0.01$ microfarad per section each wire

$l = 0.00155$ henry per section each wire

$r = 0.084$ ohm per section each wire

The values of the parameters correspond to a section of line approximately 0.73 miles long.

The Coils

Though it is possible to obtain inductance by wrapping turns into a loop, it is desirable to get the maximum inductance with the minimum amount of wire. Grover (15, pp. 94-105) derives the formulas for the maximum inductance with the different configurations for the coils. The inductance of the coil is related to the number of turns by (15, p. 98).

$$L = 0.016994 \ aN^2 \ \text{microhenrys}$$

where

a — mean radius of the turns in cms.

N — number of turns.

The copper wire #AWG 20 was used for winding the coils on a coil winder. The wire has a diameter of 0.0320 inches with double enamel insulation and a resistance of 11.1 ohms per 1000 ft. at 25° C.

The full-size coil had around 225 turns with approximately 14 layers while the half-size coils had approximately 160 turns.

The dimensions of the coils and the core are as follows:

Core: Outer diameter $= \frac{5}{16}$ inch

          Length $\qquad = \frac{12}{16}$ inch

Coils: a) full size

          number of turns = 220 - 225

          inside diameter $= \frac{15}{16}$ inch

          outside diameter $= 2 \frac{5}{16}$ inches $- 2 \frac{8}{16}$ inches

b) half size

number of turns = 160 - 170

inside diameter = $\frac{15}{16}$ inch

outside diameter = $1\frac{8}{16}$ inches

number of layers = 9 - 10

Between each pair of layers of the winding was inserted a fiber 0.015 inch in thickness for most of the coils and of 0.010 inch thickness for the remaining coils.

There were three reasons for using the fiber:

1. The fiber holds the layers in place. Without the insulation between the layers, the winding collapses after a few layers.

2. It cuts down the distributed capacitance.

3. The fiber insulates the layers one from the other in case of breakdown.

It is necessary to point out at this time that it was fairly difficult to maintain uniformity in the physical size of the coils. In the case of a full coil, for instance, the number of layers varied from 13 to 14 in order to get the same number of turns. The change in the size of the insulation from 0.015 inch to 0.010 inch in thickness made some difference in the physical dimensions.

After the insulating paper was inserted between layers and also on the last layer, the coil was taped with an electrical tape and was then wrapped with a small, narrow strip of white cloth around its radial thickness.

As explained previously, it remains quite a challenge to be able to explain exactly the behavior of the distributed capacitance of the coil. The problem is very complex when the distributed capacitance is to be known for a lightning impulse. No attempt has been made to explain that complex problem; however, it was interesting to note the behavior of the coil parameters (coil #4) at the different frequencies. To accomplish that purpose, a General Radio Twin - T Impedance Measuring Bridge type 821 - A (frequency range 460 K.C - 40 M.C) was utilized with a General Radio Standard Signal Generator type 605 B whose output was fed to the above-mentioned bridge. For the detection of the null point a model 450 - A Howard Communication receiver was used (frequency range 550 K.C - 65 M.C). The readings obtained from the Twin - T Impedance Measuring Bridge are in terms of conductance and susceptance. They were converted to the equivalent series circuit of R and L or C. Figures 8 and 9 represent the resistance and inductance or capacitance respectively with the frequency ranging from 550 kilocycles to 9.5 megacycles. It is interesting to note that the resonance point occurs at a frequency of approximately 1.1 megacycles. Below that frequency the coil acts as an inductive circuit, while at frequencies higher than resonant, coils become a capacitive circuit. The resistance at the point of resonance should theoretically be infinite, but that condition is difficult to show experimentally; however, at 1.1 megacycles (approximately the point of resonance) resistance is of the magnitude of 149,000 ohms. Another point of importance to be noted in these curves

is the phenomena around the point of resonance. The coil will offer very high impedance around the point of resonance, while it will not so obstruct the other frequencies. The coil, therefore, is equivalent to a parallel resonant circuit.

The inductance and resistance of the coils are shown in Figures 6 and 7 respectively. The d.c. resistance and the inductance at 1000 cycles were measured on a General Radio Type 650 - A Impedance Bridge. The Q of the full-size coils varied from 12.4 to 14 while 7.5 to 8.5 for the half coils.

The Capacitors

The capacitance of the capacitors used for the transmission line is shown in Figure 10. The capacitance (mica capacitors) measurements were made on a model BN capacitor bridge.

The Three Artificial Transmission Lines

The experiment was carried through by using three artificial transmission lines consisting of 14 sections each. Each section is represented by a coil and a capacitor - the values being so chosen that each section is approximately 0.73 mile long (refer to the circuit diagram of Figure 11).

It is desirable to mount the coils and capacitors in such a manner as to cut down the unnecessary mismatch by making the transmission line of tapering characteristics. In other words, if the inductance were increasing from one end of the transmission line to
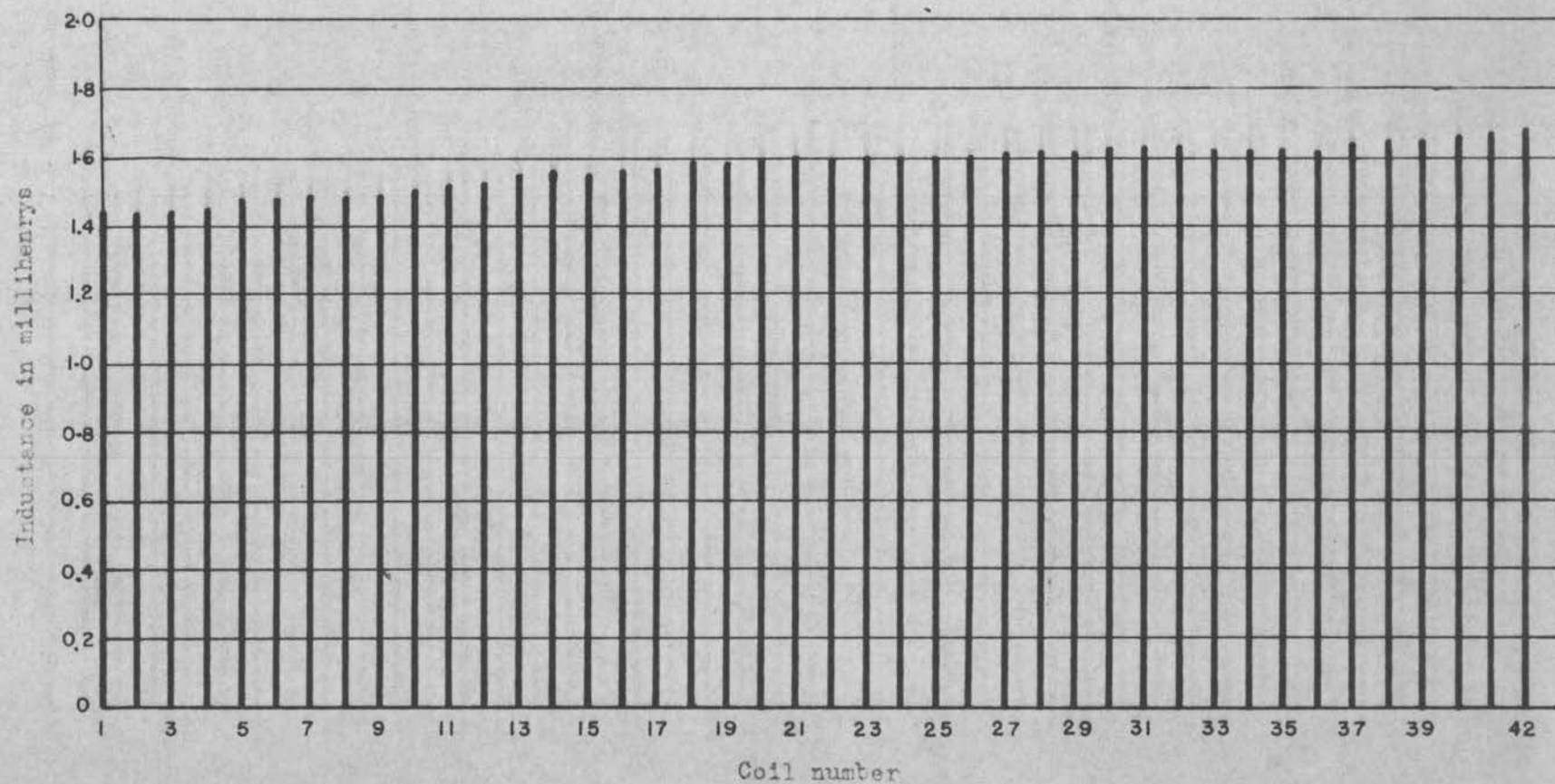
Fig. 6. The inductance in millihenrys at 1 kilocycle per second vs. coil number for the artificial transmission lines.
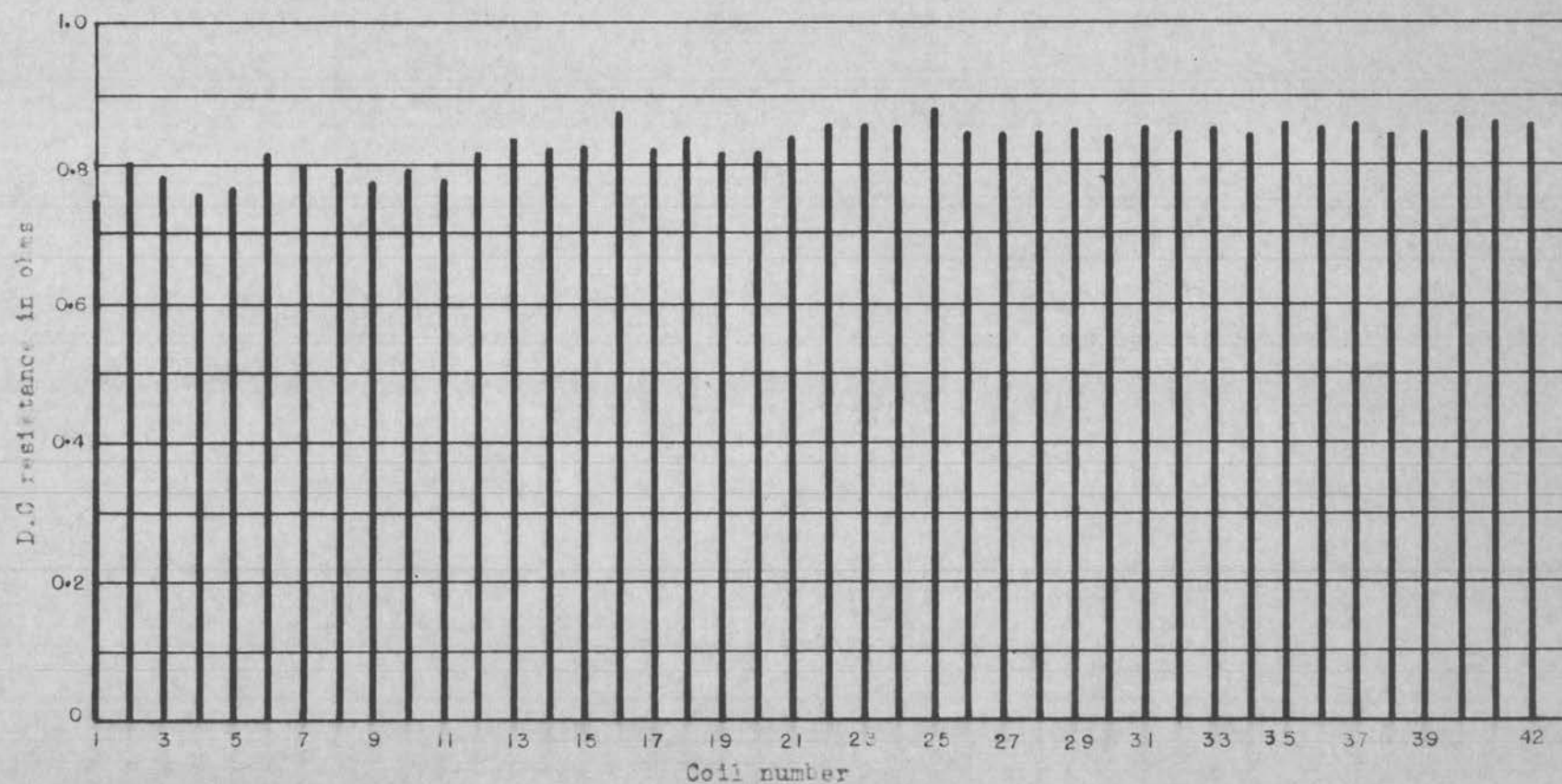
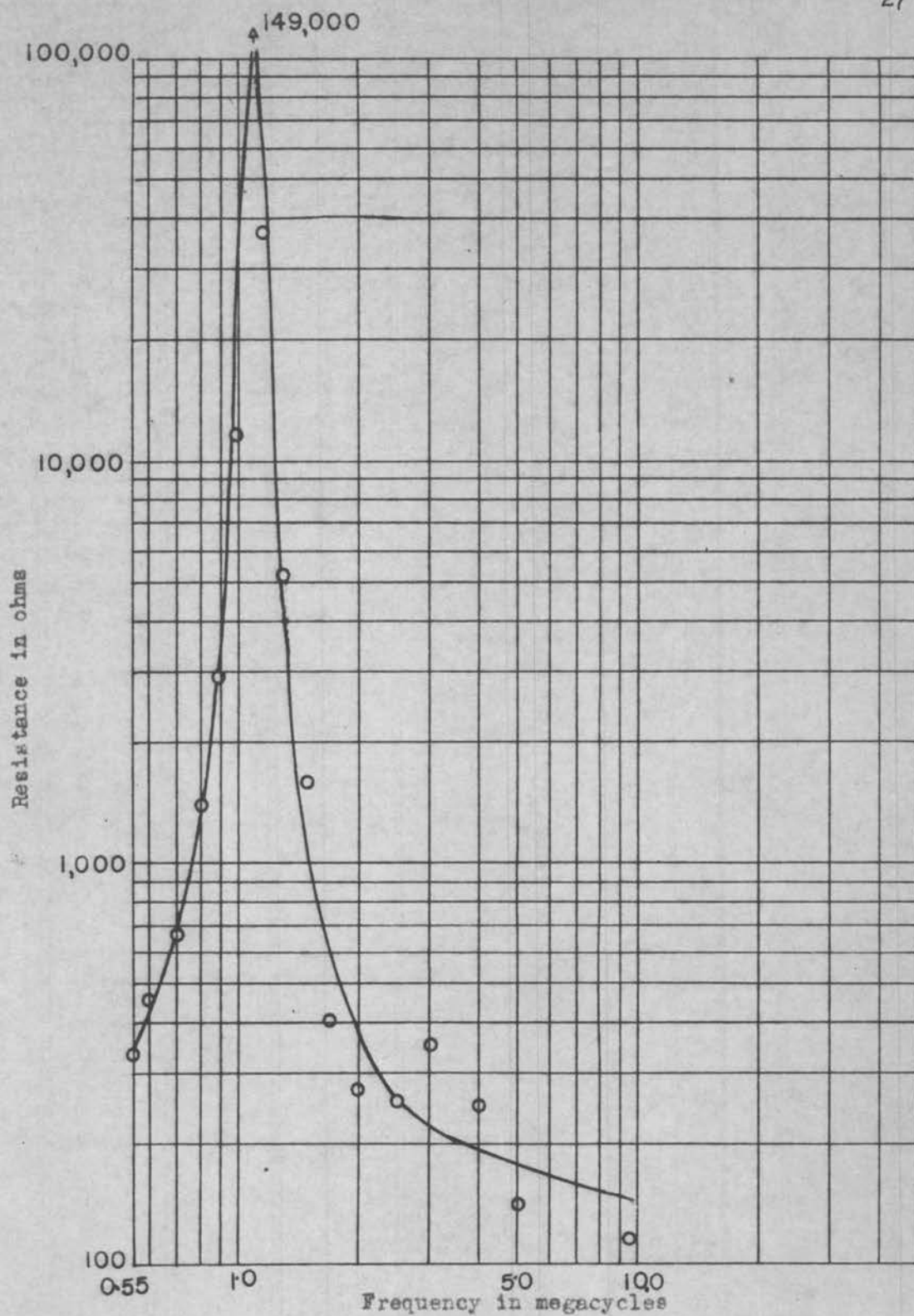Fig. 7. The D.C resistance in ohms vs. the coil number for the artificial transmission lines.

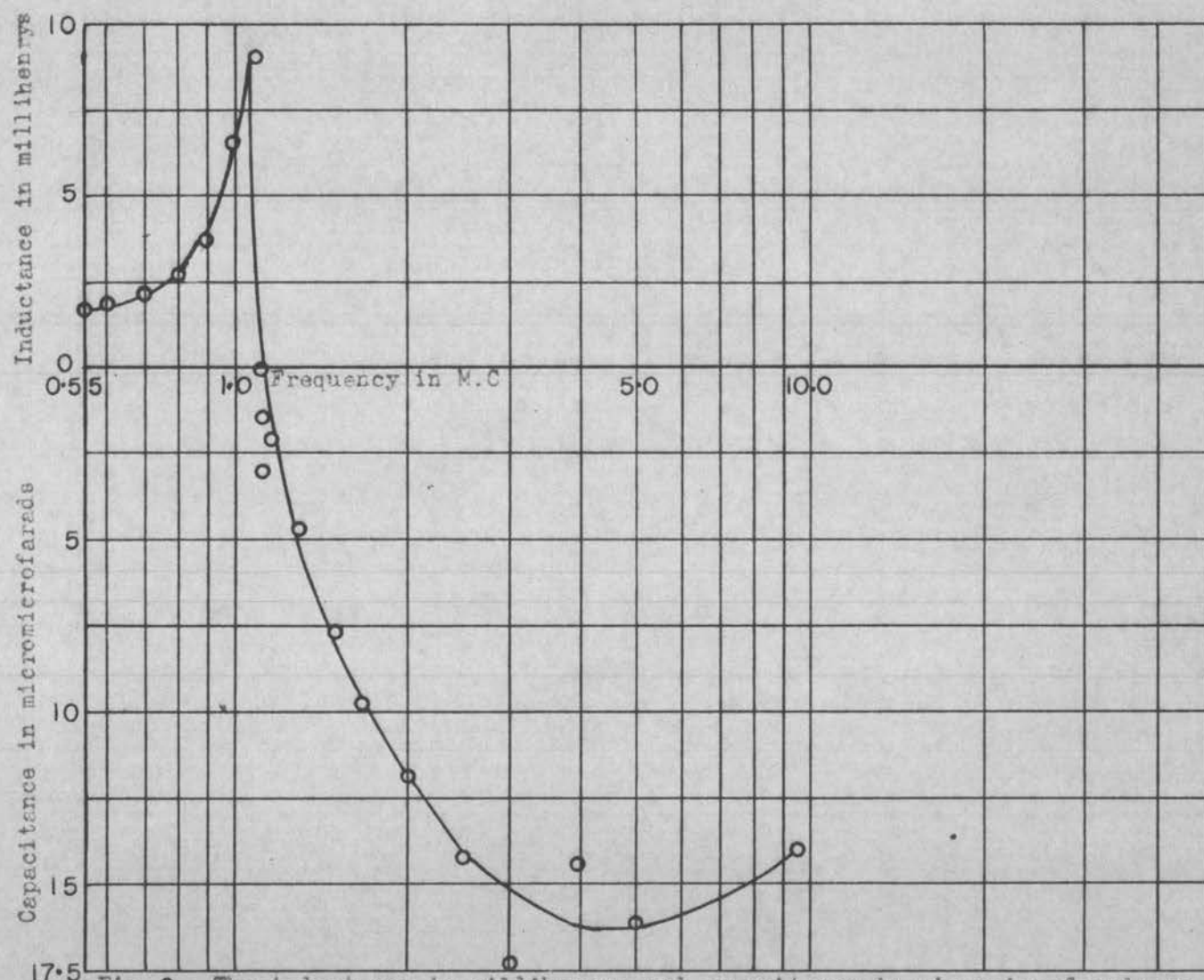Fig. 8. The resistance in ohms vs. frequency in megacycles for coil no. 26 (graph on page 25).

Fig. 9. The inductance in millihenrys and capacitance in micromicrofarads vs. frequency in megacycles for coil #26 (graph on page 25).
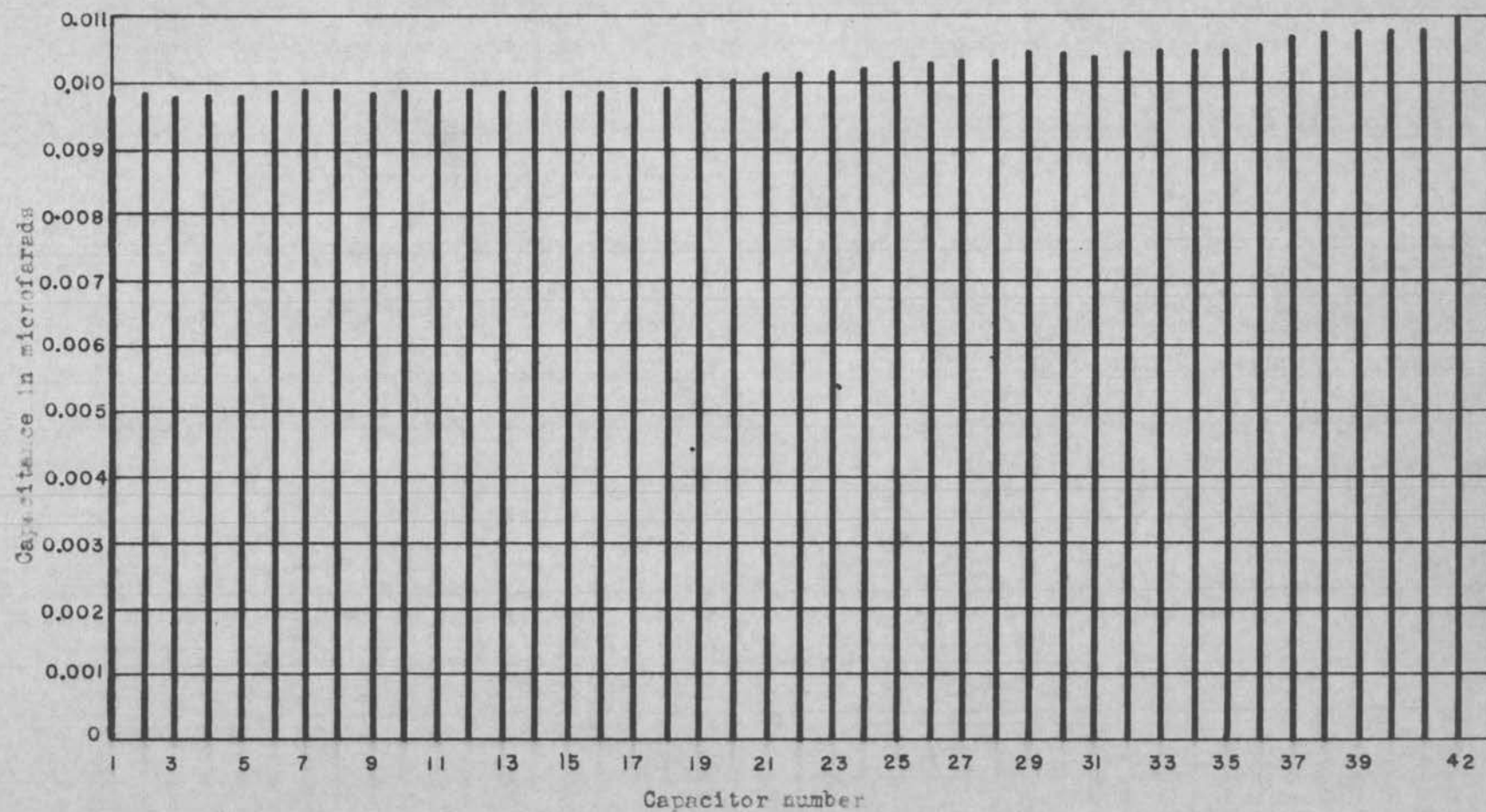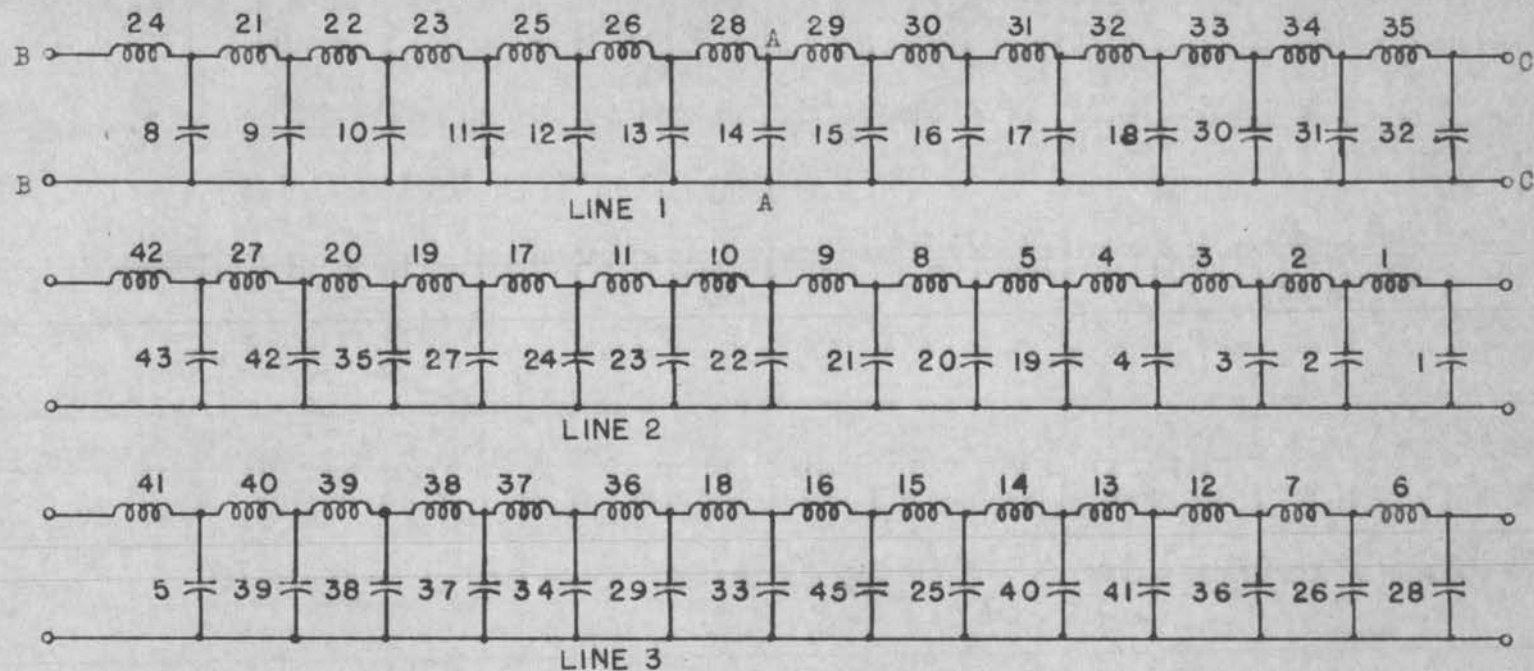
Fig. 10. The capacitance in microfarads at 60 cycles per second for the artificial transmission lines.

LINE 1

Coils: 24 21 22 23 25 26 28 (A) 29 30 31 32 33 34 35

B —o ... o— C

Capacitors: 8 9 10 11 12 13 14 15 16 17 18 30 31 32

B —o ... o— C

LINE 2

Coils: 42 27 20 19 17 11 10 9 8 5 4 3 2 1

Capacitors: 43 42 35 27 24 23 22 21 20 19 4 3 2 1

LINE 3

Coils: 41 40 39 38 37 36 18 16 15 14 13 12 7 6

Capacitors: 5 39 38 37 34 29 33 45 25 40 41 36 26 28

Key:

1) One section of a line represents 0.73 mile of an actual power transmission line.
2) The characteristic impedance is approximately 380 ohms.
3) For the values of the numbered capacitors and coils refer to pages 25 and 29.
4) The points CC are the junction points for the transmission lines.
5) The points BB or AA are the inputs.
6) When the impulse was applied at points AA, points BB were terminated in Z_o and capacitor #14 was disconnected from the line.

Fig.11. The circuit diagram for the three artificial transmission lines each consisting of 14 sections.

the other, the capacitance too should be arranged in a similar manner.
Though this principle should have been followed with more rigor, it
was observed later that the minor differences between the values
of the adjacent coils and capacitors made no difference on the wave-
shape. Table 2 shows the relationship between the numbers as they
appear on the coils and the capacitors and the numbers assigned to
them according to their values.

The mutual impedance between the coils is a problem of concern.
The coils had to be mounted in such a manner as to keep the mutual
inductance to a minimum if not reduced to zero. Actually, for a
spacing of six inches between the adjacent coils (that is how they
are mounted) the mutual inductance is not serious since the coils
are only approximately $2\frac{1}{2}$ inches in diameter. It must be kept in
mind that there are many mounting positions of the coils by which the
coupling can be reduced to a minimum. The common practice is to
mount the coils in such a way that their radial axes are perpendicu-
lar to each other, thereby cutting down the flux linkages. If the
changing magnetic flux cuts a coil at right angles, the coil will
have no induced voltages in it. Theoretically therefore it is found
that at an angle of 54° $44'$ with the axis of a coil there is locus of
points in a straight line along which there is no coupling due to the
coils (10, pp. 504-506). Since the locus is a straight line, a
series of coils parallel to each other and centered on this locus
will have no coupling. For a spacing of six inches between the
adjacent coils, the inductance measurements were made on an

impedance bridge at a frequency of 1 k.c for the coils' axes at the different positions, but no difference was noticed. At closer spacings, however, the methods of mounting coils with their axes at right angles and with the axes parallel but centered on the locus of 54° as mentioned above showed the least amount of coupling. The latter method was used for this experiment.

Table 1 indicates the voltage output at the end of each section with 10 sections of line #1 terminated in Z_0. The input to the line was a constant value of 2 volts with the frequency range of 10 kilocycles to 4 megacycles. The supply for the transmission line was taken from a Type 1001 - A Standard Signal Generator, and the voltage along the line was measured with a Hewlett Packard Model 4000 Vacuum Tube Voltmeter. It is obvious from the table that the line passes the signal without much attenuation around 10 kilocycles, while on the other hand, the output diminishes readily for frequencies around 100 k.c. At these frequencies the attenuation is quite significant even at the end of the first section.

It would have been of interest to note the voltage variations along the line at frequencies considerably above the point of resonance of the coil, but the vacuum tube voltmeters do not respond well above three or four megacycles.

By referring to the circuit diagram of the transmission line one can see that the line is equivalent to a low-pass filter. Accordingly the cut-off frequency for the line would be (5, p. 168)

Table 1. Voltage at the end of different sections with ten sections of line #1 terminated in Z_0 (Figure 11). (The input was kept constant at 2V and the frequency was varied from 10 kilocycles to 4 megacycles).

Frequency	1	2	3	4	5	6	7	8	9	10
10 k.c	2.00	2.00	1.95	1.90	1.88	1.80	1.80	1.80	1.80	1.80
15 "	2.01	2.10	2.20	2.20	2.15	2.00	1.90	1.85	1.81	1.90
20 "	1.82	1.70	1.69	1.80	1.90	1.88	1.70	1.52	1.47	1.58
30 "	1.78	1.95	2.00	1.80	1.70	1.70	1.85	1.65	1.30	1.40
40 "	2.10	2.10	1.70	1.80	1.90	1.40	1.50	1.70	1.20	1.20
50 "	2.16	1.75	1.78	1.70	1.30	1.62	1.10	1.35	1.20	0.88
60 "	1.99	1.60	1.70	1.25	1.42	1.00	1.20	0.75	0.92	0.50
70 "	1.80	1.35	1.46	1.10	0.90	1.00	0.75	0.60	0.70	0.30
80 "	1.60	1.20	0.98	0.80	0.60	0.45	0.40	0.36	0.26	0.08
90 "	1.00	0.50	0.24	0.13	0.07	0.03	0.01	0.00	0.00	0.00
100 "	0.64	0.21	0.06	0.02	0.00	0.00	0.00	0.00	0.00	0.00
200 "	0.10	0.00	0.00	0.00						
.										
.										
.										
.										
.										
4 m.c	0.00									

$$f_c = \frac{1}{\pi (LC)^{1/2}} = \frac{1}{\pi (1.6 \times 10^{-3} \times 0.01 \times 10^{-6})^{1/2}} = 79.5 \text{ kilocycles/second.}$$

Such, however, is not the case. Were it so, the lightning impulse (consisting of frequency components much higher than 79.5 kilocycles) would lose much of its steepness even at the end of the first section. Therefore, the only other explanation is that the distributed capacitance of the coil changes the line characteristics to some extent. The distributed capacitance of the coil will tend to pass some of the frequency components which the coil inductance will not normally pass. The limitation to the passage of the signal will occur around the resonant point of the coil, and it will offer very high impedance. For frequencies above resonance, again the distributed capacitance might offer a low impedance path; consequently, it can be summarized that at frequencies considerably below and above the point of resonance, the windings offer low impedance while at resonance, they have very high impedance (22, pp. 1030-1040).

It should be noticed that at frequencies far above resonance the shunt capacitors offer quite low impedance and hence the output diminishes quite readily. Consequently the line is a low-pass filter, but the cut-off frequency is not as described above.

With reference to Table 1, another question of interest arises. Why is it that the magnitude of the voltage along the line does not keep on decreasing as it moves farther away from the source? At the different sections of the line, the voltage is higher than the preceding sections. It cannot be due to the small variations in the

values of the adjacent coils and capacitors because the voltage
irregularities are not consistent at all times at any particular
point. It cannot be due to the effect of the distributed capacitance
because we are dealing with frequencies far below the point of
resonance and the coil is essentially an inductor (Figure 9). It is
possible, however, that the characteristic impedance of the line
might be different at the different frequencies, thereby causing
standing waves along the line.

The Comparison of Voltage Waveforms with T and π Formation of the Line

Figure 12 shows the voltage waveforms along transmission line
#1 with the impulse applied to it through a full coil, a half coil
or a capacitor (0.01 microfarads). The voltage waveform at the
sending end is quite smooth for a full coil, while it shows some
oscillations for a half coil; the oscillations become quite pre-
dominant at the wavefront for a capacitor. These are the
oscillations which make a current waveform even more oscillatory
according to the relationship $i = c \frac{dv}{dt}$. Though the oscillations
become predominant for all three cases at the end of the first
section, the case of the capacitor is the worst around the wavefront.
The use of the full coil at the input of line, therefore, was fully
justified. Since the transmission lines consist of only full coils
and full capacitors with the coils preceding the capacitors, the use
of words T or π is immaterial
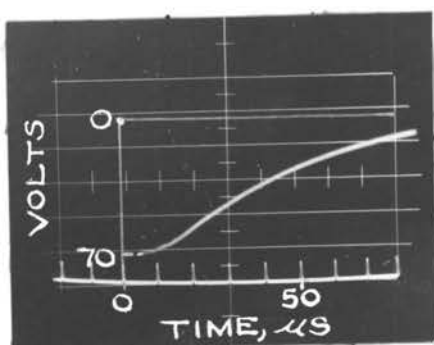
a) The sending end voltage for
   the full coil.
   Total time - 100 microseconds
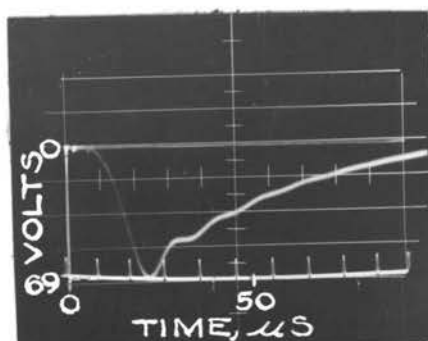
b) The voltage at section 1 for
   the full coil.
   Total time - 100 microseconds
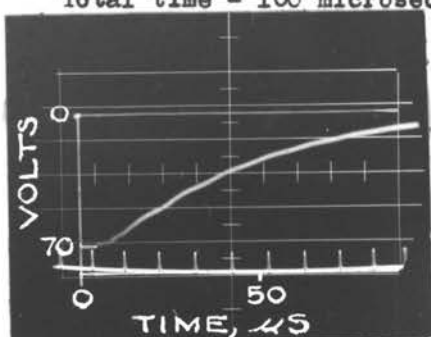
c) The sending end voltage for
   the half coil.
   Total time - 100 microseconds
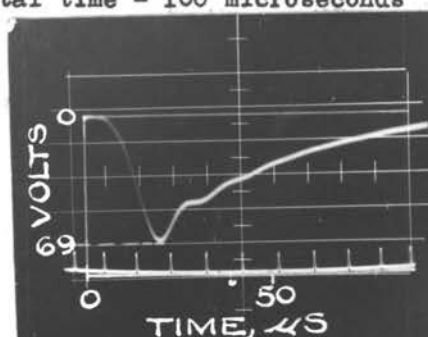
d) The voltage at section 1 for
   the half coil.
   Total time - 100 microseconds
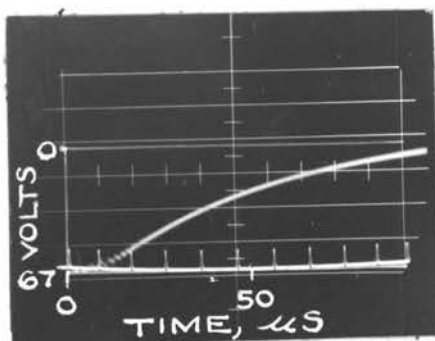
e) The sending end voltage for
   a capacitor.
   Total time - 100 microseconds
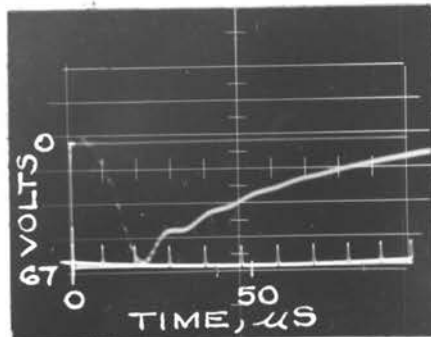
f) The voltage at section 1 for
   the capacitor.
   Total time - 100 microseconds

Fig.12. The voltage waveforms along transmission line #1 (figure 11)
with the impulse applied to it through a full coil, a half
coil or a capacitor. The transmission line #1 was termi-
nated in Z_0 at points CC.

The Voltage and Current Waveforms Across a Full
Coil, a Half Coil and a Capacitor

It was found useful to apply an impulse directly to a full coil,
a half coil, and a capacitor individually and study their character-
istics. The period of oscillation for the full and the half coil is
approximately 80 microseconds for both the current and the voltage
waveforms (Figure 13). The current waveform across the capacitor
is complex and is difficult to photograph. The oscillations are so
predominant that the waveform was invisible with both the high or
the low gains of the oscilloscope. The current waveform shown was
taken with a high gain of the oscillograph and with a total time of
3,000 microseconds. It is to be assumed that even the minimum amount
of inductance in the circuit can cause noticeable oscillations.

The Voltage and Current Waveforms Along the
Artificial Transmission Line

All the current and voltage waveforms dealt with have their time
axes ranging from zero on the left side of the oscillograms to
maximum on the right side. The peak magnitudes of the current and
the voltage waveforms are labeled for all the oscillograms.

Figures 14 and 15 show the voltage waveforms along the transmis-
sion line at the end of the different sections when the line was
terminated in its characteristic impedance (to be discussed below).
The applied impulse was a standard 1.5/40 microseconds waveform as
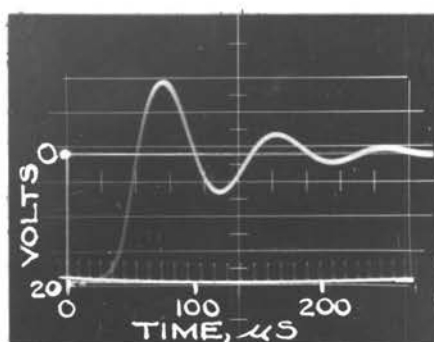
a) The voltage waveform across
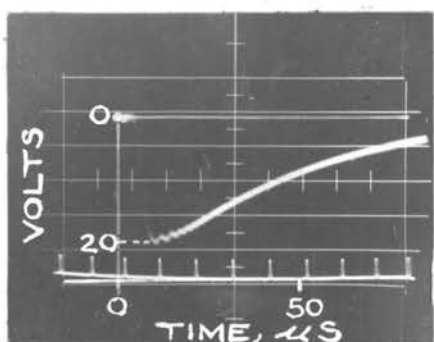the full coil.
Total time - 300 microseconds
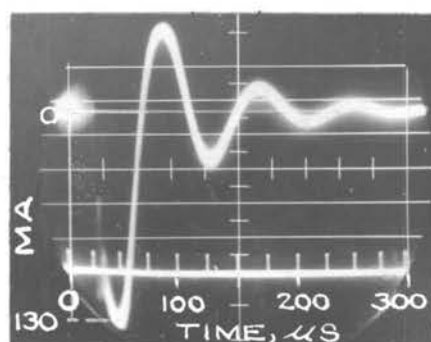
b) The current waveform through
a full coil.
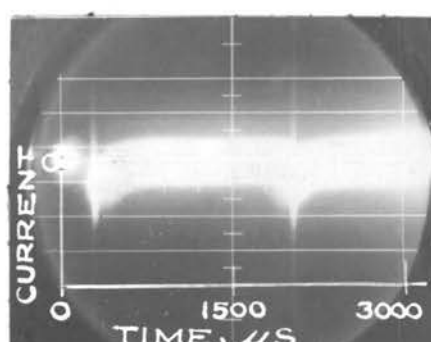Total time - 300 microseconds
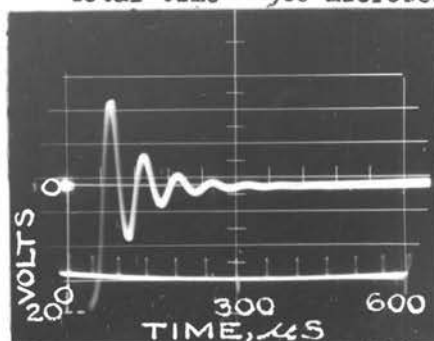
c) The voltage waveform across
the half coil.
Total time - 600 microseconds
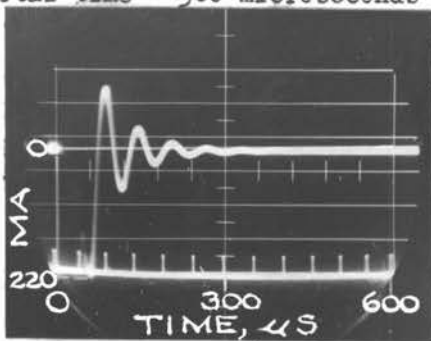
d) The current waveform through
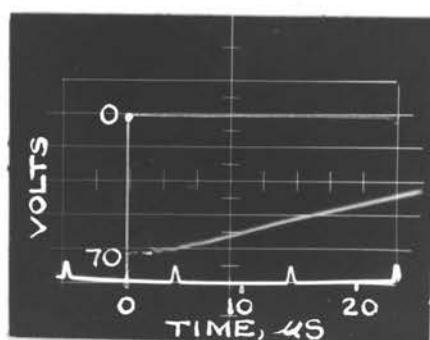the half coil.
Total time - 600 microseconds

e) The voltage waveform across the
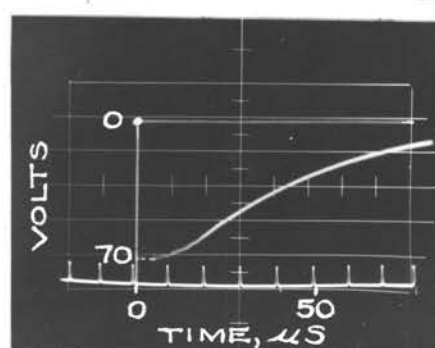capacitor.
Total time - 100 microseconds

f) The current waveform through
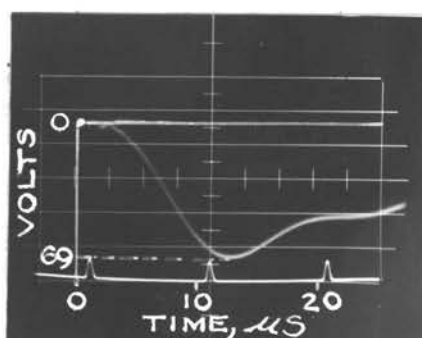the capacitor.
Total time - 3000 microseconds

Fig. 13. The voltage and current waveforms across a full coil, a
half coil and a capacitor when a standard 1.5/40 micro-
seconds impulse was applied to them.

a) The sending end voltage.
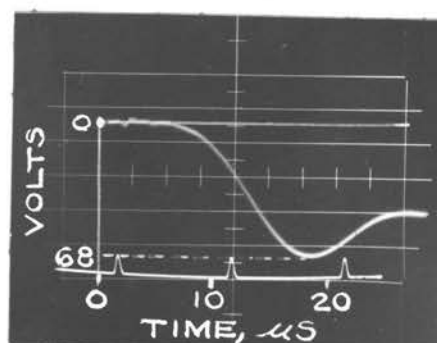   Total time - 30 microseconds

b) The sending end voltage.
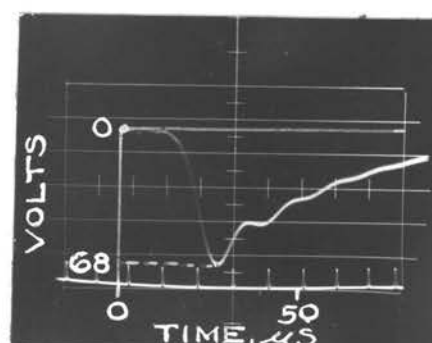   Total time - 100 microseconds

c) The voltage at section 1.
   Total time - 30 microseconds
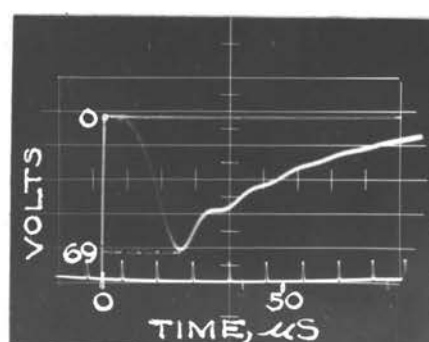
d) The voltage at section 1.
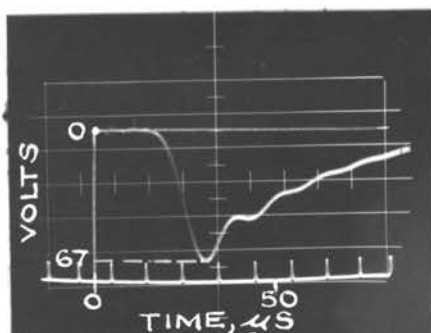   Total time - 100 microseconds

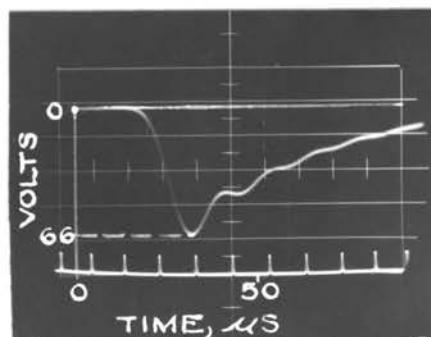e) The voltage at section 2.
   Total time - 30 microseconds

f) The voltage at section 2.
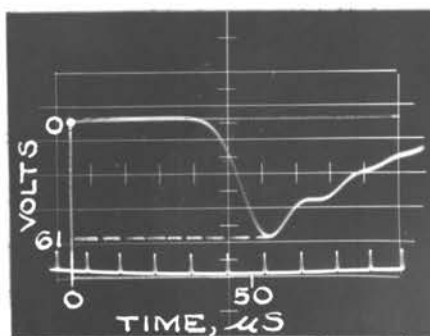   Total time - 100 microseconds

Fig. 1. The voltage waveforms along the transmission line with 42
        sections terminated in the characteristic impedance.
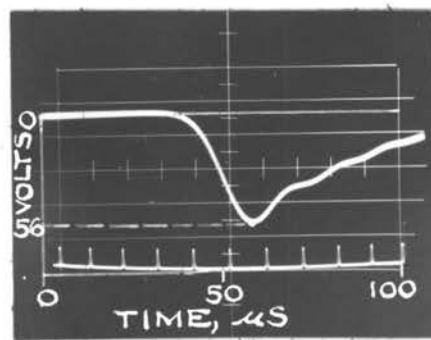   The impulse was applied at points BB of figure 11.

a) The voltage at section 3.
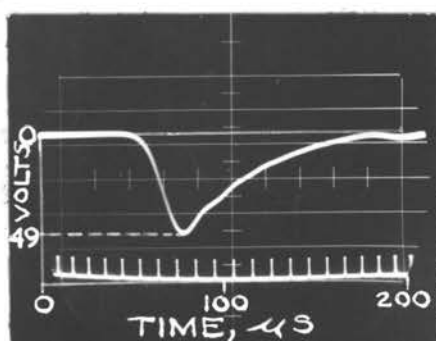   Total time - 100 microseconds

b) The voltage at section 5.
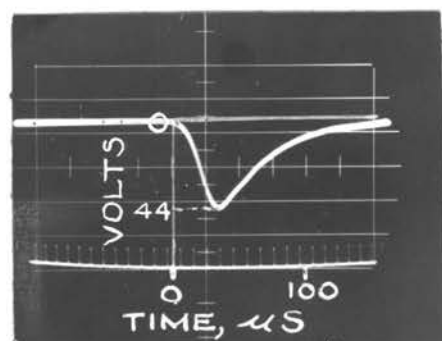   Total time - 100 microseconds

c) The voltage at section 10.
   Total time - 100 microseconds

d) The voltage at section 14.
   Total time - 100 microseconds

e) The voltage at section 28.
   Total time - 200 microseconds

f) The voltage at section 42.
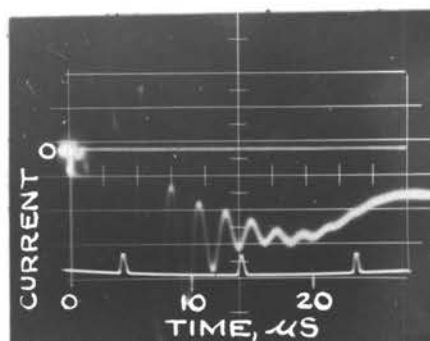   Total time - 300 microseconds

Fig.15. The voltage waveforms along the transmission line with 42
sections terminated in the characteristic impedance. The
impulse was applied at points BB of figure 11.

shown on Figures 14 a and b with a peak magnitude of 70 volts. In
order to show the rising portion of the waveforms the scale was
expanded to 30 microseconds while a total scale of 100 microseconds
was used commonly to show the wavetails. Also, the scale was reduced
to more than 100 microseconds quite often to show the results in an
appropriate form.

At the end of section 1, the wavefront has been attenuated and
distorted to approximately 11 microseconds (The expression wavefront
of 11 microseconds means that it takes 11 microseconds for the
impulse to rise from its initial zero point to its peak value.) while
the wavetail is of the duration of about 45 microseconds. There is
no appreciable change in the peak magnitude of the voltage waveform.
By the time the impulse arrives at the end of section 2, the wave-
front becomes 14 microseconds and the wavetail shows no appreciable
change from the previous section except that the oscillations in
the waveform become pronounced. Even now the peak magnitude of the
waveform shows no noticeable attenuation. The waveform at the end
of five sections shows that the wavefront and the wavetail is still
about the same. The peak magnitude of the waveform is reduced to
about 66 volts from its initial value of 70 volts peak. At this
point, it is of interest to compare the results with an actual power
transmission line. When lightning strikes a power transmission
line the high surge voltages cause corona which in turn is the
controlling factor for the attenuation and distortion of the
traveling waves and consequently the magnitude of the impulse

decreases faster than it would on the artificial transmission line. However, the distortion produced by the artificial transmission line is quite noticeable. The wavefront is 11 microseconds even during the first section and 17 microseconds at the end of 5 sections (little more than three and a half miles). At the end of 10 sections, the wavefront is 20 microseconds and the peak magnitude has decreased to about 61 volts. As the waveform has traveled 14 sections (approximately 10 miles), the wavefront peaks at 23 microseconds and the wavetail has a duration of over 50 microseconds. The peak magnitude is roughly 56 volts. The waveform shows a wavefront of about 30 microseconds and a wavetail of nearly 60 microseconds at the end of 28 sections. The magnitude is about 49 volts. By the time the impulse has traveled about 30 miles (as represented by 42 sections) its wavefront lasts for about 34 microseconds, the wavetail for about 70 microseconds and the magnitude has gone down to nearly 44 volts. Figure 22 shows a graph of the steepness and the peak magnitude of the wavefront as it progresses along the line. It can be concluded that though the wavefront and wavetail are attenuated and distorted as the impulse travels along the line and the magnitude continues to decrease, the wavefront is distorted the most at the first few sections of the artificial transmission line.
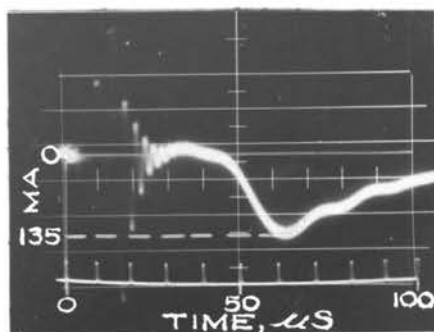
Figure 16 shows the current waveforms along the transmission line with 42 sections terminated in the characteristic impedance. The applied impulse was of the same nature as for the last figures which show the voltage waveforms. In order to measure or record
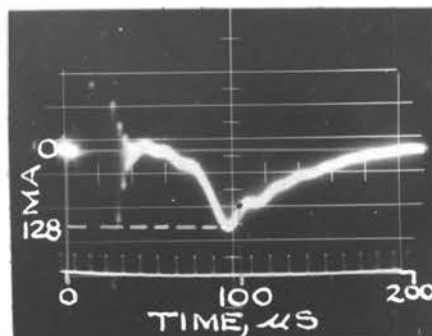
a) The sending end current.
   Total time – 30 microseconds
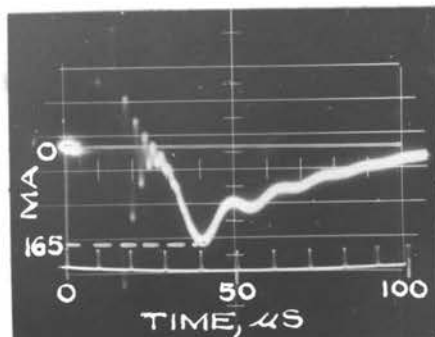
b) The current at section 5.
   Total time – 100 microseconds

c) The current at section 10.
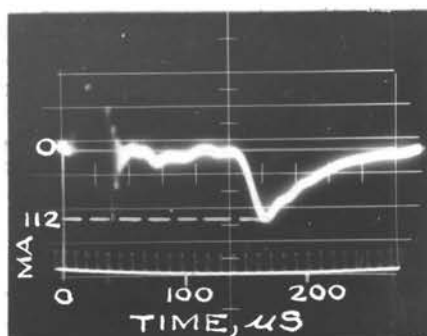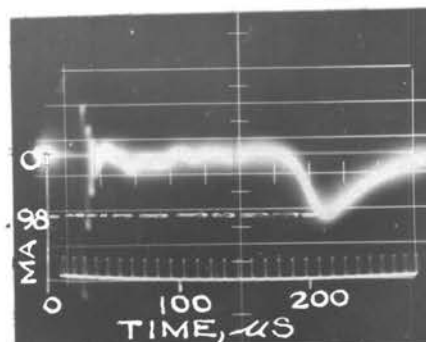   Total time – 100 microseconds

d) The current at section 14.
   Total time – 200 microseconds

e) The current at section 28.
   Total time – 300 microseconds

f) The current at section 42.
   Total time – 300 microseconds

Fig. 16. The current waveforms along the transmission line with
42 sections terminated in the characteristic impedance.
The impulse was applied at points BB of figure 11.

the current waveforms without disturbing the system, a resistor of
1 ohm was inserted on the ground side of the line wherever the current
waveform was desired. To make sure that there were no inductance
due to the resistor, the resistor itself was a straight wire of high
resistivity with a length of only a few inches.

It is interesting to point out that although smooth voltage
waveforms can be produced by changing the generator constants the
current waveforms are not so simple as that. Though we deal quite
frequently with the voltage waveforms to study the surge phenomena,
the current waveforms seem to be kept mostly for theoretical
purposes. Since we are dealing with capacitors and coils, the
oscillations are secondary. No attempt has been made in this paper
to determine the oscillations or their period as related to the trans-
mission lines or the coils. The facts are presented as observed and
the compromises are made as pointed out in the last paragraph.

Since it was hard to determine the magnitude, wavefront, and
the wavetail at the sending end of the current waveforms of Figure
16, a smooth 1.5/40 microseconds voltage impulse was applied at the
sending end, and the current waveforms were observed along the line.
Each vertical division on the graticules of the oscillogram
corresponds to 30 milliamperes for this figure. At the end of
five sections, the current has a magnitude of approximately 165
milliamperes. As the current waveform reaches 10 sections, its
magnitude has decreased to 135 milliamperes. Similarly the current
waveform has gone down to 128 milliamperes at the end of 14 sections

to 112 milliamperes at the end of 28 sections and to 98 milliamperes at the end of 42 sections.

From the oscillograms it is obvious that the wavefront and the wavetail are attenuated and distorted as the impulse travels along the line. The wavefront lasts for 30 microseconds and the wavetail for 55 microseconds at the end of 10 sections. As the impulse has traveled approximately 10 miles (14 sections) the wavefront peaks at 35 microseconds and the wavetail has a duration of 65 microseconds. At the end of 28 sections, the wavefront is 40 microseconds and the wavetail lasts for 70 microseconds. The wavefront and wavetail last for 45 and 75 microseconds respectively at the end of 42 sections (about 30 miles).

It is interesting to notice the time an impulse takes to travel some distance on an artificial transmission line. The experiment was conducted by applying an impulse to the transmission line at one end and watching the waveform at the desired point under investigation. The time which the impulse took to travel from the sending end to the point of investigation showed as a straight line on the oscilloscope. As a matter of fact, all the waveforms shown have a straight line at the beginning of the impulse. With reference to Figure 1 it can be seen that the triggering impulse (shown in Figure 21) serves two purposes; first, it fires FG-33 which results in the production of the impulse and secondly, it triggers the sweep on the oscilloscope. It can be seen then that the triggering impulse sets up a reference time for all the waveforms on the oscilloscope. Because of the ionization time (which is only few microseconds)

of the thyratron FG-33, the results at the end of first few sections
cannot be relied on; however, at the end of 14, 28 and 42 sections,
the average time of travel per section came out to be approximately
4 microseconds. This compares reasonably well with 982 feet per
microsecond (equivalent to 3.92 microseconds per section of the
artificial transmission line)--the velocity of light.

<div align="center">

The Voltage Waveforms with Different Terminations
### For the Artificial Transmission Line

</div>

When a transmission line is terminated in its characteristic
impedance, there are no reflections from the load end; the voltage
and current waveforms are fully absorbed by the load. Though special
care is taken to match the line impedance and the load impedance for
communication works, such is not the case on power transmission lines
because of the uncertainty of the load. The load on the power lines
may vary from very small values of Z_0 up to almost an open circuit.
Therefore, it is useful to investigate the surge phenomena for both
above-mentioned extremes of the load.

When a transmission line is open circuited at the far end, the
wave travels along the line suffering the usual distortion and
attenuation and is reflected from the open end without any reversal
of sign; it doubles in magnitude as compared to what it would have
been if the line were terminated in its characteristic impedance.
The current waveform on the other hand is reflected from the open
end with a reversal of sign thus leaving zero resultant current at
the open end.

For the case of a transmission line with the far end short cir-
cuited, the conditions are the opposite of those in the open-circuit
conditions. The voltage waveform is reflected with a reversal of
sign, hence leaving zero resultant voltage at the receiving end. The
current waveform on the other hand is reflected from the short-
circuited end without any reversal of signs and therefore the current
magnitude doubles.

Figure 17 shows the voltage waveforms along the artificial
transmission line #1 with different terminations. In these pictures
the scale is reduced to show the reflections. By observing the
voltage waveform at the sending end with the far end open circuited,
one can see that the reflections of the waveform from the far end
reach the sending end while the first waveform is still being sent
from the generator. This is quite logical because the total dura-
tion for a standard 1.5/40 microseconds waveform is well over 100
microseconds and the time for a wave to travel to and from 14
sections is approximately 112 microseconds. The voltage waveform
at the end of 10 sections with line open circuited shows quite an
interesting phenomenon. Since the traveling time from section 10
to section 14 and back is only about 32 microseconds, the reflected
wave arrives at the 10th section and adds to the voltage waveform
thereby giving that added magnitude to the voltage as seen on the
oscillogram. The voltage at the end of 14 sections is doubled with
the end open circuited as can be seen by the comparison of the
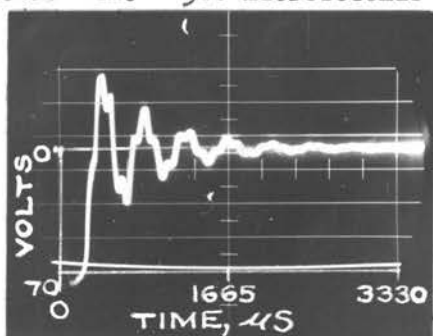waveform of Figure 17 c with the waveform of Figure 15 d. The
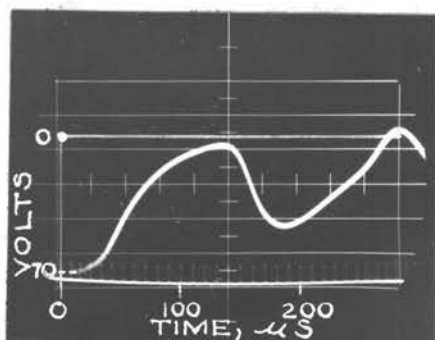
a) The sending end voltage with
   line open circuited.
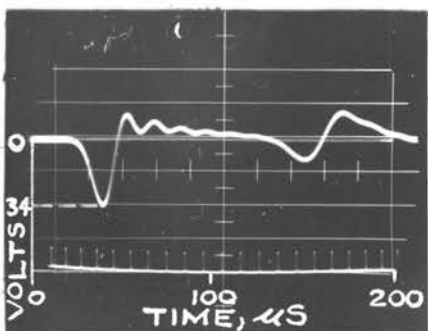   Total time - 300 microseconds
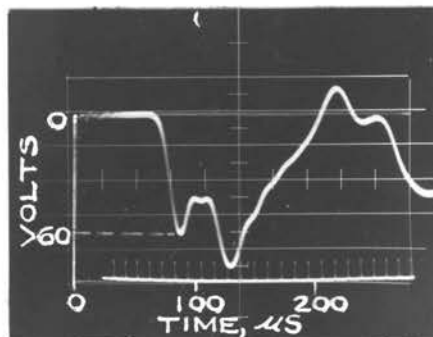
b) The voltage at section 10 with
   line open circuited.
   Total time - 300 microseconds
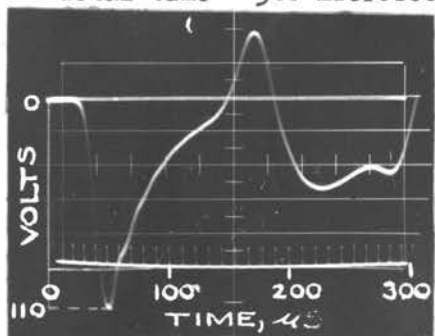
c) The voltage at section 14 with
   line open circuited.
   Total time - 300 microseconds.

d) The sending end voltage with
   line short circuited.
   Total time - 3330 microseconds

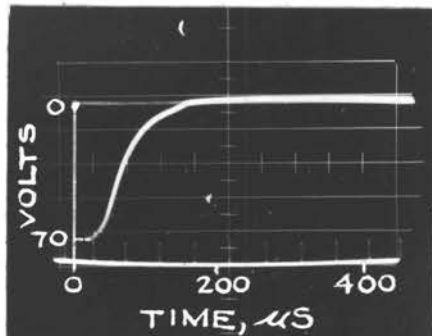e) The voltage at section 13
   with line short circuited.
   Total time - 200 microseconds

f) The sending end voltage with
   line terminated in Z_0.
   Total time - 500 microseconds

Fig.17. The voltage waveforms along transmission line #1 with
        different terminations. The impulse was applied at
        points BB of figure 11.

positive portion of the waveform in Figure 17 c indicates that the voltage waveform is reflected from the sending end with a reversal of sign because the impedance of the generator is lower than the characteristic impedance of the line.

The oscillogram of the sending end voltage with the line (Figure 11) short circuited is shown on a total time of 3330 microseconds in order to show the reflections in detail. The reflections continue back and forth until they are completely absorbed by the transmission line. One notices that with a negative-sending-end voltage waveform, the first reflection registered at the generator side of the transmission line is positive because negative voltage is reflected from the short-circuited end with a positive polarity. The second registered reflection is negative because the previously received positive waveform is reflected without sign reversal (because the generator side of the line has higher impedance than the short-circuited side of the transmission line) which in turn is reflected back from the short-circuited side with a reversal of polarity. This process continues until the waveforms are reduced to zero in magnitude. The similar reasoning can be applied for the voltage waveform at the end of 13 sections with line short circuited. Though the voltage at section 14 is zero, such is not the case for section 13 because of the time of delay between these adjacent sections.

In order to obtain the characteristic impedance of the transmission line (refer to Figure 17 f) the voltage waveform was watched

at the sending end for no reflections while the non-inductive
resistor was varied at the far end. The Z_0 thus used to eliminate
reflections was approximately 380 ohms.

In order to obtain the impedance of the generator the line was
open circuited and a variable non-inductive resistor was inserted
in series with the line next to the generator. The series resistor
was varied until the reflections (not the first reflection) were
eliminated. The difference between the characteristic impedance and
the series resistor gave the impedance of the generator which for
this particular part of the experiment came out to be roughly 20 ohms.

The Surge Phenomena at the Transition Points of the Artificial Transmission Lines

The Waveforms and the Discussion

The transition point on the transmission line can be referred
to as the abrupt change of circuit constants, such as open- or
short-circuited terminal, or a junction with another line, or a
transformer or a machine winding. In this experiment the only
transition point due to transmission lines is considered. This study
owes its importance to the power transmission line substations where
several lines form a point of transition. Consider the case of a
lightning impulse striking a line a few miles away from a substation;
the traveling waves are set up on each side of the transmission line.
The reflections which follow will depend on the nature of the
impedance offered to both ends of the transmission line. This study

deals with the above-mentioned simulation whereby the lightning impulse was applied at points AA (Figure 11) of transmission line #1, points BB were terminated in Z_0 and points CC were treated as the points of junction with different terminations.

To produce a standard lightning impulse at points AA of Figure 11, the generator constants had to be changed (as explained below) from the previous setting used for applying the standard impulse at points BB. For example, to produce a standard 1.5/40 microseconds voltage waveform at point BB, the generator constants (Figure 1) were as follows:

C_1 - 0.05 and 0.03 microfarads in series

R_1 - 10 ohms

R_2 - 2000 ohms

C_2 - 0.10 microfarads

With the same generator constants, the impulse wavetail did not last for 40 microseconds when applied at points AA. The new generator constants were as follows:

C_1 - 0.05 and 0.03 microfarads in series

R_1 - 5.5 ohms

R_2 - 1000 ohms (R_2 did not make much difference)

C_2 - 0.2 microfarads

The value of C_2 had to be doubled while R_2 was lowered. For the first case the generator has to feed only one line while for the second case the impulse is fed to two lines. For the latter case, the higher value of C_2 holds the wavetail for a longer time because

of its longer time constant, or, to look at it from another point of view, because it stores more energy.

To produce a standard impulse at the generator without any load applied to it, the value of C_1 was made higher as compared to the previous cases, the value of C_2 was made lower and the values of R_1 and R_2 were kept about the same. The value of C_1 had to be reduced to keep the wavefront sharp (1.5 microseconds) when the load was added to the generator.
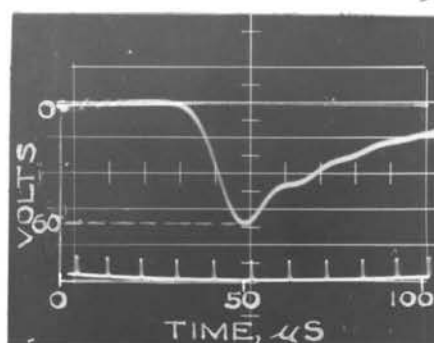
Figure 18 shows the voltage waveforms along transmission line #1 and at the junction CC with different terminations. The voltage at the junction with Z_0 termination or with a line added is the same. This is obvious from the fact that as the waveform reaches point CC, it sees the characteristic impedance of the line. Later, however, reflections may occur if the line at the far end is not properly terminated.

When at the junction of Figure 11, line #2 and line #3 are added, the voltage magnitude at the junction is reduced to 40 volts as compared to 60 volts with only Z_0 at the junction. It was interesting to study the effect of $\frac{Z_0}{2}$ termination at the junction. As is obvious from the oscillograms, it gave the same results as if the line at the junction were terminated in two lines of the same characteristic impedances.
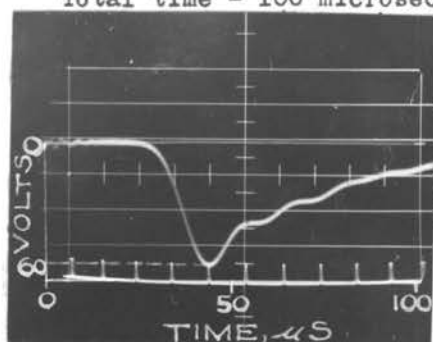
The voltage magnitude at the junction with Z_0 and line #2 and line #3 reduced in magnitude to 31 volts which is approximately half of the value when the junction had only Z_0 as its termination. The
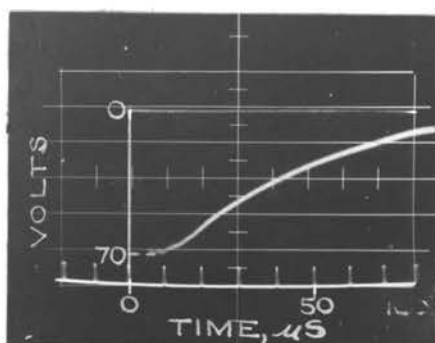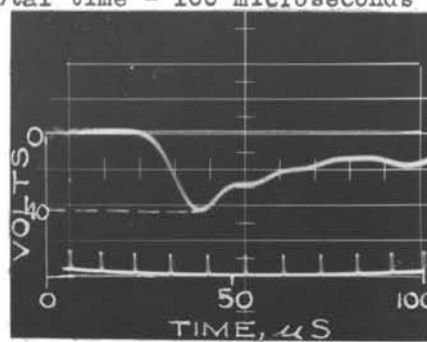
a) The sending end voltage with points CC terminated in Z_O. Total time - 100 microseconds
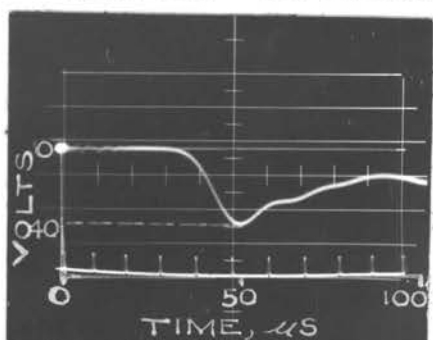
b) The voltage at the junction with Z_O termination. Total time - 100 microseconds

c) The voltage at the junction with only line #2 added. Total time - 100 microseconds

d) The voltage at the junction with lines #2 and #3 added. Total time - 100 microseconds

e) The voltage at the junction with $\frac{Z_O}{2}$ only. Total time - 100 microseconds
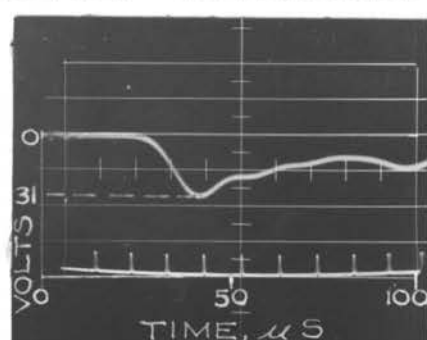
f) The voltage at the junction with Z_O plus lines #2 and #3. Total time - 100 microseconds

Fig. 18. The voltage waveforms along transmission line #1 and at the junction CC with different terminations. The impulse was applied at points AA and the line at points BB (figure 11) was terminated in Z_O.

combination of Z_0 and lines #2 and #3 is equivalent to three lines at the junction with a fourth line as the line on which the impulse arrives.

The current waveforms at the junction with different terminations are shown in Figures 19 and 20. They correspond to the voltage waveforms discussed in the previous paragraphs. The current at the junction of line #1 with Z_0 termination has a magnitude of 38 milliamperes which is the same as for the junctions terminated in another line. The current at the junction on line #1 has a current magnitude of about 50 milliamperes (approximately 4/3 of the previous case) when two lines come to the junction of line #1. The current magnitude remains the same if instead of two lines coming to a junction an impedance $\frac{Z_0}{2}$ is used as the termination for line #1. The current magnitude at the junction on line #1 increases to 56 milliamperes (roughly one and a half times as much when the junction was terminated in Z_0) when lines #2 and #3 and Z_0 are used as the terminations at the junction. For the above case the current on lines #2 and #3 is nearly 19 milliamperes (roughly 1/2 of the 38 milliamperes at the junction on line #1 when the junction was terminated in Z_0) at the junction.

Figures 23 and 24 represent the current and voltage magnitudes in per unit values respectively as the number of outgoing lines are increased at the junction of Figure 11. The per-unit value of 1.0 indicates the voltage or the current magnitude at the junction when the incident line is terminated in its characteristic impedance.

a) The sending end current with points CC terminated in Z_0. Total time - 100 microseconds

b) The current on line #1 at the junction with Z_0 termination. Total time - 100 microseconds
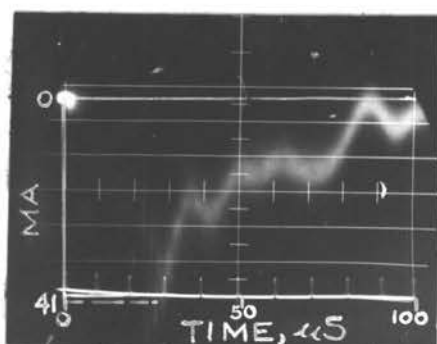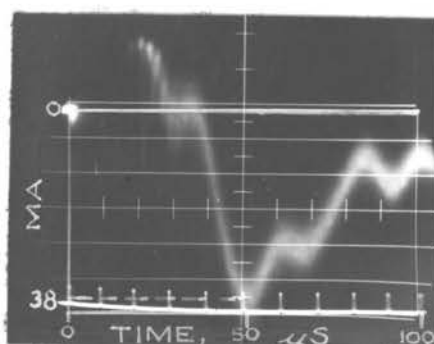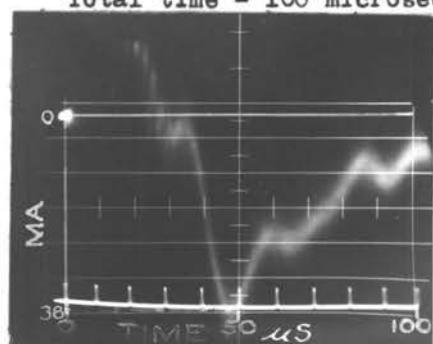
c) The current on line #1 at the junction with only line #2 added. Total time - 100 microseconds
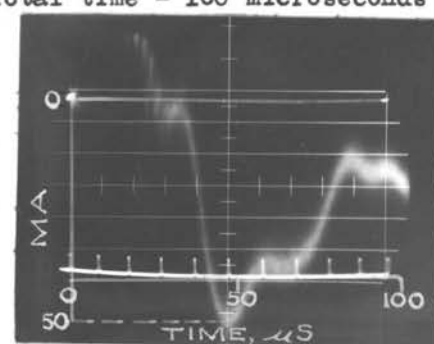
d) The current on line #1 at the junction with lines #2 and #3 added. Total time - 100 microseconds
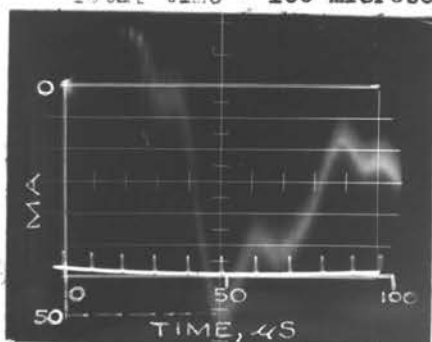
e) The current on line #1 at the junction with $Z_0/2$ termination only. Total time - 100 microseconds
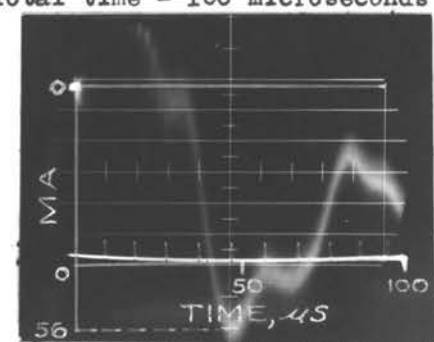
f) The current on line #1 at the junction with Z_0 plus lines #2 and #3. Total time - 100 microseconds

Fig. 19. The current waveforms along transmission line #1 and at the junction CC with different terminations. The impulse was applied at points AA and the line at points BB (figure 11) was terminated in Z_0.
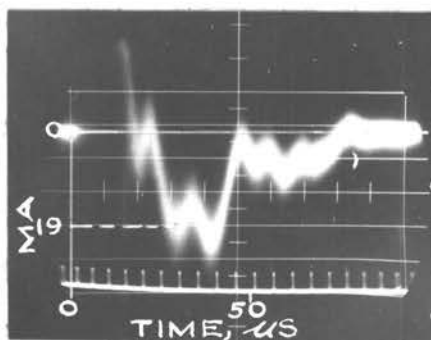
a) The current on line #2   b) The current on line #3
   Total time – 100 microseconds   Total time – 100 microseconds
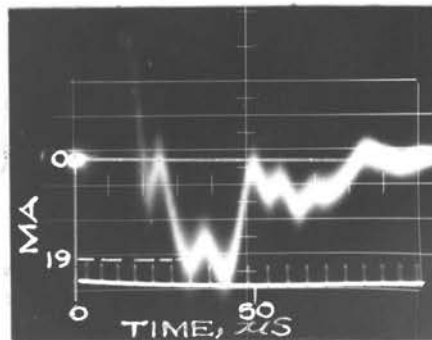
Fig.20. The current waveforms on the lines #2 and #3 (figure 11)
        at the junction with Z_o plus lines #2 and #3.

Fig.21. The triggering impulse from
        the output of thyratron 884
        for the thyratron FG-33
        (figure 1).
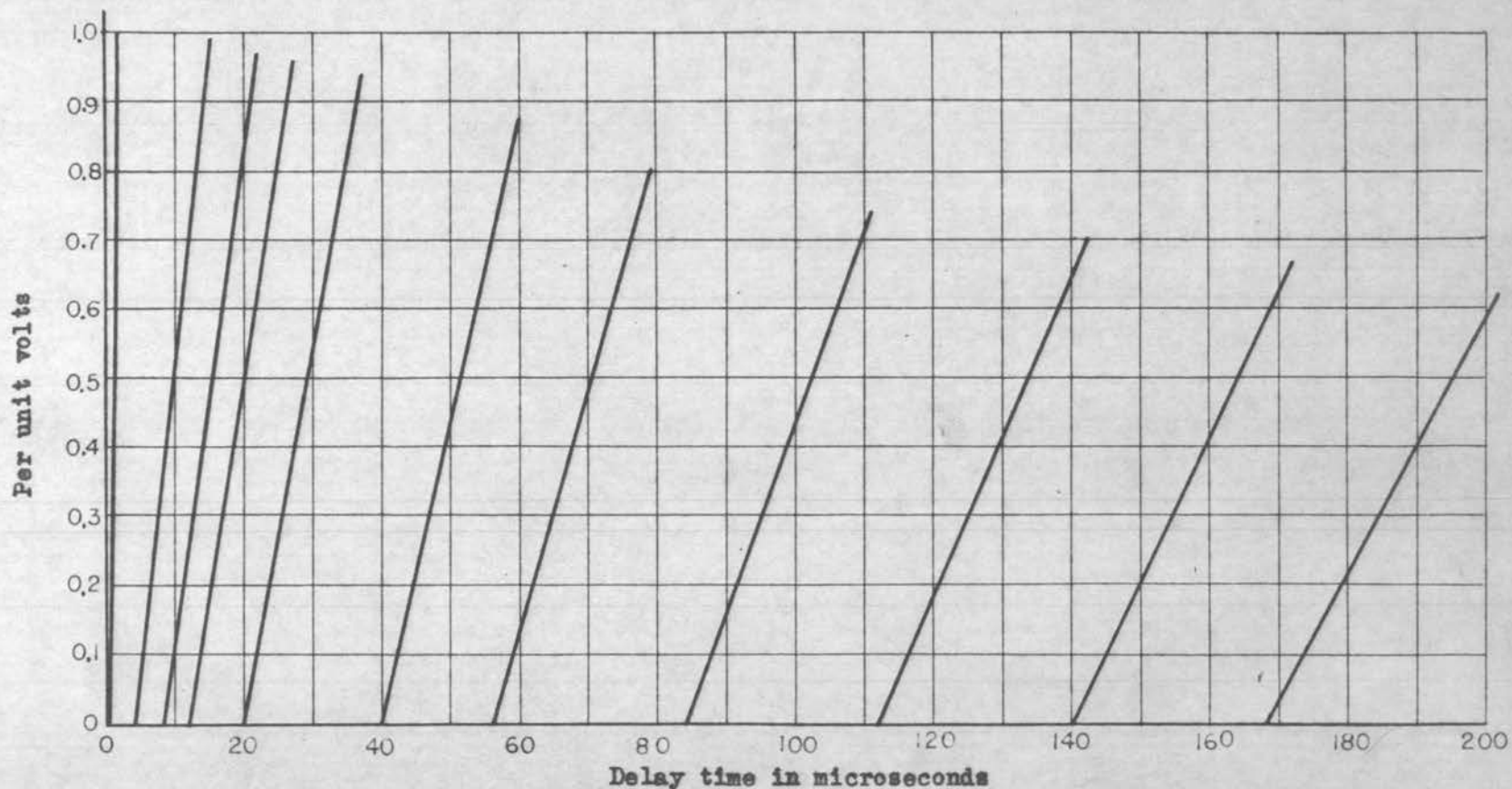
Fig. 22. The volts in per-unit values vs. delay time in microseconds for the wavefront as it progresses along the line. The slanted lines show the steepness and the magnitude of the wavefront corresponding to a particular point along the line.
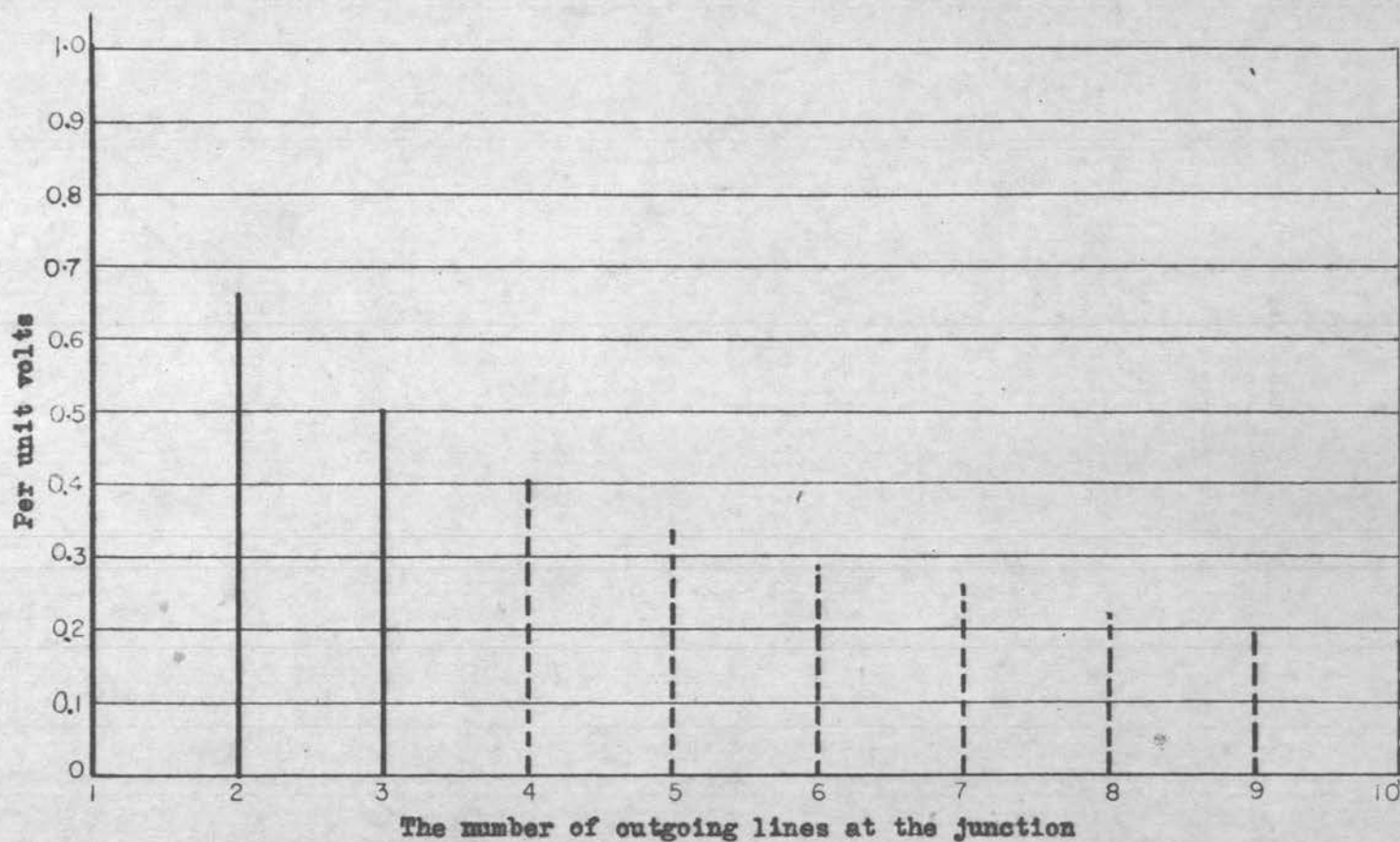
Fig. 23. The volts in per-unit values at the junction (points CC of figure 11) as the number of outgoing lines is increased. The 1.0 per unit value of voltage corresponds to a single line terminated in Z_0 at the junction.
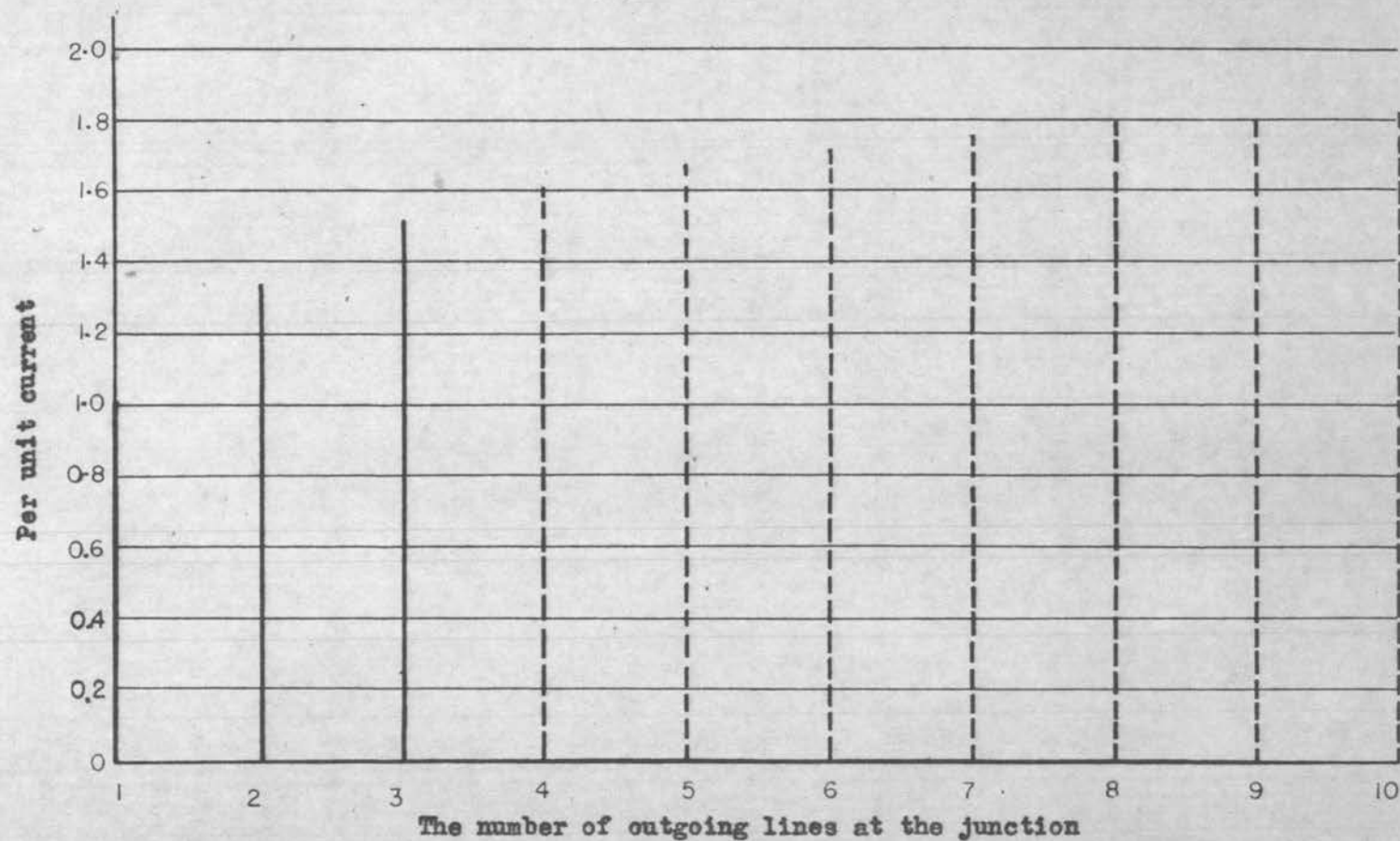
Fig. 24. The current in per-unit values at the junction (points CC of figure 11) as the number of outgoing lines is increased. The 1.0 per unit value of current corresponds to a single line terminated in Z_0 at the junction.

The solid lines indicate the experimental results while the dotted lines represent the theoretical values up to 10 outgoing lines from a substation.

The voltage magnitude at the junction decreases quite rapidly at first and then diminishes gradually as the number of lines are increased. The current magnitude on the incident line, on the other hand, increases with increasing lines at a junction. The decrease in the voltage magnitude and the increase in the current magnitude at the junction is due to the decreasing value of the equivalent impedance with the increasing number of transmission lines. As the impedance of the termination gets smaller than the characteristic impedance of the line the voltage wave is reflected with a reversal of polarity, thereby decreasing the initial value, and the current waveform is reflected without a reversal of polarity thereby increasing the initial value of the current.

The Mathematical Analysis of the Waveforms at the Junction

With reference to Figure 11 points CC are made the reference points for the computations. The incident voltage and current waveforms on line #1 are related by Z_1 (the characteristic impedance of line #1) such that (1, pp. 40-42)

$$\frac{e_1}{i_1} = Z_1 .$$

The reflected waves (shown by a single prime) are related by the negative of the surge impedance

$$\frac{e_1'}{i_1'} = Z_1 \ .$$

The transmitted waves (shown by double prime) on outgoing lines are related by

$$\frac{e_k''}{i_k''} = Z_k \ . \quad (Z_k = Z_1 \text{ for all the lines})$$

The total current and voltage at the transition point are

$$i_0 = i_1 + i_1'$$

$$e_0 = e_1 + e_1' = Z_T i_0 \ , \quad Z_T \text{ is the equivalent impedance of the outgoing lines (not including line \#1).}$$

From the above relationships,

$$e_1' = \frac{Z_T - Z_1}{Z_T + Z_1} \, e_1 = \text{reflected voltage wave}$$

$$e_0 = \frac{2 \, Z_T}{Z_T + Z_1} \, e_1 = \text{total voltage}$$

$$i_1' = - \frac{Z_T - Z_1}{Z_T + Z_1} \, i_1 = \text{reflected current wave}$$

$$i_0 = \frac{2}{Z_T + Z_1} \, e_1 = \text{total current}$$

$$i_k'' = \frac{e_0}{Z_k} = \frac{2 \, Z_T}{Z_T + Z_1} \cdot \frac{e_1}{Z_k} = \text{current wave transmitted to any line k.}$$

$$e_k'' = e_0 = i_k'' Z_k = \frac{2 \, Z_T}{Z_T + Z_1} \cdot \frac{e_1}{Z_k} \cdot Z_k = \frac{2 \, Z_T}{Z_T + Z_1} \cdot e_1$$

$$= \text{voltage wave transmitted to any line k.}$$

In order to compare the experimental and the theoretical results one may consider first the case of the junction when it is terminated by two outgoing lines.

The total voltage at the junction is

$$e_0 = \frac{2 Z_T}{Z_T + Z_1} e_1 = \frac{2}{3} e_1 \text{ because } Z_T = \frac{Z_1}{2}.$$

The total current is

$$i_0 = \frac{2}{Z_T + Z_1} \cdot e_1 = \frac{4}{3} \frac{e_1}{Z_1} \text{ (}\frac{4}{3} \text{ of the current if the line were terminated in } Z_0\text{)}.$$

For the case of two lines and Z_0 as the outgoing lines, the total voltage at the junction is

$$e_0 = \frac{2 Z_T}{Z_T + Z_1} e_1 = \frac{e_1}{2}, \text{ because } Z_T = \frac{Z_1}{3}$$

The total current is

$$i_0 = \frac{2}{Z_T + Z_1} e_1 = \frac{3}{2} \frac{e_1}{Z_1} \text{ (}\frac{3}{2} \text{ of the current if the line were terminated in } Z_0\text{)}.$$

The current transmitted to any outgoing line is

$$i''_k = \frac{e_0}{Z_k} = \frac{2 Z_T}{Z_T + Z_1} \cdot \frac{e_1}{Z_k} = \frac{e_1}{2 Z_1} \text{ (}\frac{1}{2} \text{ of the current if the line were terminated in } Z_0\text{)}.$$

and is equivalent to 1/3 of the total current.

The experimental and theoretical results are in good agreement.

It can be summarized very briefly that the voltage magnitude at the junction with two outgoing lines is reduced to 2/3 of its original value while the current magnitude increases to 4/3 of its

initial value (the initial value refers to the conditions of Z_0 termination at the junction). With two outgoing lines and Z_0 at the junction, the voltage is reduced to half of its initial value while the current jumps to one and one half of its original value. The current transmitted to the outgoing lines for the above case is 1/2 of the initial value of the current at junction on line #1 when it is terminated by Z_0 only.

64

SUMMARY AND CONCLUSIONS

It is possible to study the surge phenomena on the artificial
transmission lines with a miniature surge generator. Since the surge
generator puts out an impulse with every cycle a stationary pattern
of the voltage and current waveforms can be observed on the oscillo-
scope. By changing the generator constants, one can achieve quite a
variety of waveforms.

The artificial transmission lines can pass the standard
lightning impulses though the wavefront is distorted and attenuated
even during the first section. The distributed capacitance of the
coils plays an important role in the behavior of the waveform along
the line.

Since appreciably higher voltages can be developed at the open
ends of the transmission line, it is desirable to avoid such condi-
tions on a substation. On the other hand, currents of higher magni-
tude are developed at the short-circuited ends of the transmission
lines.

The influence of the multiple lines at the junction is to reduce
the surge voltage at that transition point. As the number of lines
at the transition point increases, the voltage magnitude is lowered.
As for the current waveforms, the current at the junction on the
incident line increases in magnitude because of the reflections with-
out any reversal of signs when many lines come together at the junction.

It can be concluded that the simulated apparatus in the laboratory gives satisfactory results which can give a fair idea of the actual happenings in the field.

BIBLIOGRAPHY

1. Bewley, L. V. Traveling waves on transmission systems. 2d ed. New York, John Wiley, 1951. 543p.

2. Birmingham power station. Testing 132 KV cable insulation. Electrician 139:684-5. September 5, 1947.

3. Cage, John M. Theory and applications of industrial electronics. New York, McGraw-Hill, 1951. 290p.

4. Craggs, J. D. and J. M. Meek. High voltage laboratory technique. London, Butterworths, 1954. 404p.

5. Creamer, Walter J. Communication networks and lines. New York, Harper, 1951. 353p.

6. Daves, C. L., C. H. Thomas and A. B. Drough. The measurement of impulse voltages by repeated-structure networks. Transactions of the American institute of electrical engineers 69:571-583. 1950.

7. Davis, W. L. and C. E. Warren. The calibration of ignition crest voltmeters. Transactions of the American institute of electrical engineers 66:99-104. 1947.

8. Dellenbaugh, Jr., F. S. Artificial transmission lines with distributed constants. Transactions of the American institute of electrical engineers 42:803-23. 1923.

9. Edwards, F. S., A. S. Husbands and F. R. Perry. The development and design of high-voltage impulse generators. The proceedings of the institution of electrical engineers A98:155-180. May 1951.

10. Everitt, W. L. Communication engineering. New York, McGraw, 1932. 567p.

11. Gross, I. W., L. B. Levesconte and J. K. Dillard. Lightning protection in extra-high-voltage stations-influence of multiple circuits. Transactions of the American institute of electrical engineers. III. Power apparatus and systems. 72:885-890. 1953.

12. Gross, I. W., and G. D. McCann. Field investigation of lightning surges at substations. Transactions of the American institute of electrical engineers 66:569-576. 1947.

13. Gross, I. W., T. J. Bliss and J. K. Dillard. A study of light-
    ning protection in extra-high-voltage stations. Transac-
    tions of the American institute of electrical engineers.
    III. Power apparatus and systems 71:482-492. 1952.

14. Gross, I. W., et al. High voltage impulse tests in substations.
    Transactions of the American institute of electrical
    engineers. III-A. Power apparatus and systems 73:210-220.
    1954.

15. Grover, Frederick W. Inductance calculations. 2d ed. New
    York, D. Van Nostrand, 1947. 286p.

16. Harder, E. L. and J. M. Clayton. Lightning phenomenon.
    Westinghouse engineer, July 1951. pp. 106-111.

17. Harder, E. L. and J. M. Clayton. Lightning problems solved
    with the synchronograph. Transactions of the American
    institute of electrical engineers. III. Power apparatus
    and systems 72:376-383. 1953.

18. Monaham, T. F. A note on the impulse testing of power trans-
    formers. Proceedings of the institution of electrical
    engineering. 2. Power engineering 100:35-37. 1953.

19. Moran, J. H. Impulse testing without delay. Allis-Chalmers
    electrical review, fourth quarter, 1950. pp. 10-12.

20. Moses, Graham Lee and R. J. Alke. Studies of impulse strength
    and impulse testing problems on high-voltage generators.
    Transactions of the American institute of electrical
    engineers. III. Power apparatus and systems 72:123-131.
    1953.

21. Recommendations for impulse voltage testing. Transactions of
    the American institute of electrical engineers 52:466-474.
    1933.

22. Rudenberg, Reinhold. Performance of traveling waves in coils
    and windings. Electrical engineering 59:1030-1040. 1940.

23. Skilling, Hugh Hildreth. Electric transmission lines. New York,
    McGraw, 1951. 438p.

24. Terman, Frederick Emmons. Radio engineers handbook. New York,
    McGraw, 1943. 1019p.

68

25. Thomason, J. L. Impulse generator circuit formulas. Transactions of the American institute of electrical engineers 53:169-176. 1934.

26. Thomason, J. L. Impulse generator voltage charts for selecting circuit constants. Electrical engineering 56:183-189. 1937.

27. Wagner, C. F., I. W. Gross and B. L. Lloyd. High voltage impulse tests on transmission lines. Transactions of the American institute of electrical engineers. III-A. Power apparatus and systems 73:196-209. 1954.

28. Woodruff, L. F. Principles of electric power transmission. 2d. ed. New York, Wiley. 1949. 257p.

APPENDIX

APPENDIX

The mathematical analysis for the basic impulse generator circuit of Figure 25.

For the derivation of the equations given below, refer to reference 9, pp. 117-129.

The following equations deal with the discharge of C_1 (once it has been charged through different sources) through R_1, R_2 and C_2.

The general equation of the voltage waveform across the output resistor is of the form:

$$v = A \left[e^{-(\alpha - \beta)t} - e^{-(\alpha + \beta)t} \right].$$

The time to peak is determined by setting $\frac{dv}{dt} = 0$ and solving for t which then is the time t_1 to peak value and is given by

$$t_1 = \frac{1}{2\beta} \log_e \left(\frac{\alpha + \beta}{\alpha - \beta} \right).$$

The peak value of the voltage, therefore, can be written as

$$v_{max} = A \left[e^{-(\alpha - \beta)t_1} - e^{-(\alpha + \beta)t_1} \right].$$

The voltage then decreases to half the peak value in a time t_2, so that

$$A \left[e^{-(\alpha - \beta)t_2} - e^{-(\alpha + \beta)t_2} \right] = \frac{1}{2} A \left[e^{-(\alpha - \beta)t_1} - e^{-(\alpha + \beta)t_1} \right].$$

The value of t_2 can be expressed only in terms of ratios of the different parameters including t_1.

The constants A, α and β are given as follows

$$A = V_0 C_1 R_2 \frac{\alpha^2 - \beta^2}{2\beta}$$, V_0 is the voltage to which C_1 is initially charged.

$$\alpha = \frac{R_2 C_2 + R_1 C_1 + R_2 C_1}{2\,C_1 C_2 R_1 R_2}$$

$$\beta = \frac{1}{2}\left\{\left(\frac{R_2 C_2 + R_1 C_1 + R_2 C_1}{C_1 C_2 R_1 R_2}\right)^2 - \frac{4}{C_1 C_2 R_1 R_2}\right\}^{\frac{1}{2}} .$$
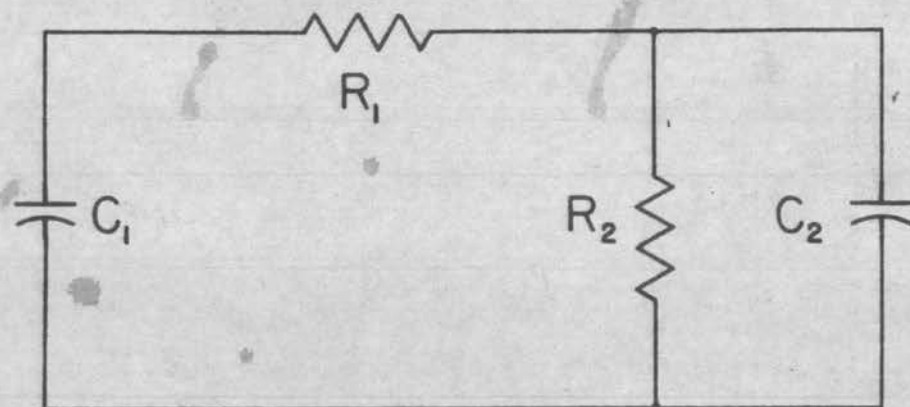
C_1 – generator capacitance

R_1 – series resistor

R_2 – shunt resistor

C_2 – load capacitance

Fig. 25. The basic impulse generator circuit.

Table 2. The relationship between the numbers as they appear on the coils and the capacitors and the numbers as assigned to them according to their values (Graphs of Figures 6 and 10, respectively).

Actual Coil No.	Coil No.'s on graphs		Actual Capacitor No.	Capacitor No.'s as shown on the graphs
42	1		1	1
43	2		14	2
34	3		12	3
45	4		2	4
41	5		C-23	5
22	6		C-22	6
8	7		1	7
32	8		2	8
44	9		3	9
33	10	bigger	4	10
40	11	(physically)	5	11
19	12	size	6	12
2	13	capacitors	7	13
7	14		8	14
17	15		9	15
28	16		10	16
38	17		11	17
6	18		12	18
35	19		C-21	19
39	20		C-20	20
3	21		C-19	21
1	22		C-18	22
5	23		C-16	23
23	24		C-15	24
27	25		C-17	25
4	26		C-13	26
36	27		13	27
29	28		C-14	28
31	29		C-12	29
21	30		9	30
11	31		4	31
15	32		7	32
14	33		C-8	33
18	34		C-10	34
13	35		C-11	35
24	36		C-9	36
25	37		C-7	37
10	38		C-6	38
16	39		C-5	39
26	40		C-4	40
9	41		C-3	41
37	42		3	42
			15	43
			C-1	44
			C-2	45